Aeolian Research 15 (2014) 113–132

Contents lists available at ScienceDirect

Aeolian Research

journal homepage: www.elsevier.com/locate/aeolia

Geochemical archive in the three loess/paleosol sections in the Eastern Croatia: Zmajevac I, Zmajevac and Erdut

L. Galović *

Croatian Geological Survey, Sachsova 2, 10001 Zagreb, Croatia

ARTICLE INFO

Article history:
Received 2 April 2014
Revised 23 July 2014
Accepted 29 July 2014
Available online 2 September 2014

Keywords:
Loess
Paleosol
Geochemistry
Trace elements
REE
Croatia

ABSTRACT

The loess record in the Eastern Croatia provides an excellent high-resolution archive of climate and environmental change, providing evidence for the interaction between accumulation and erosion of aeolian and fluvial sediments during the Middle and Late Pleistocene. Impressive loess–paleosol successions up to 30 m thick are exposed by neotectonic movements along SE slope of the Bansko Brdo (=Bansko Hill) (Zmajevac I and Zmajevac) and the steep cliffs of the Danube River (Erdut). The published lithostratigraphical results are complemented by geochemical studies (content of major, trace and REE and pH). In Zmajevac I section three paleosols are intercalated in the loess, in Zmajevac four and in Erdut four paleosols are intercalated in the loess. IRSL age estimates of 17.8 ± 1.9 and 217 ± 22 ka indicate that most of the middle and upper pleniglacial loess record is missing. In all investigated sections, alluvial sediments are intercalated in the loess deposits, indicating periods of fluvial activity. Geochemical characteristics of investigated paleosols explain both the main characteristics and degree of pedogenesis. Paleosol horizons could be clearly distinguished from loess based content of major, trace and REE and on weathering coefficients, such as Ba/Sr and $(CaO+Na_2O+MgO+K_2O)/Al_2O_3$.

1. Introduction

Quaternary alluvial, marshy and lake sediments are widespread in Eastern Croatia (Figs. 1 and 2). They are mostly overlain by aeolian-derived sediments, e.g., loess, that were formed during the cold periods of the Pleistocene. Some paleosols, which were formed during more humid and warmer periods of the Pleistocene, are intercalated in the loess. In the study area, two main processes cause exposures of loess sections: neotectonic elevation of Bansko Brdo and the Danube River erosion of loess sediments forming steep cliffs along the Danube River. These loess successions are excellent archives of climate change, entailing environmental change, during the Middle and Late Pleistocene time periods (Galović et al., 2009, 2011; Újvári et al., 2014; Marković et al., 2009, 2011).

Loess research in Croatia extends back to the beginning of the 20th century. The famous "Gorjanović Profile" situated on the west of the Danube River has been extensively investigated for about 100 years by means of mineralogical, paleontological, chronological, geomorphological, pedological and climatological studies (Gorjanović-Kramberger, 1912, 1914; Bronger, 1976, 2003; Rukavina, 1983; Galović and Mutić, 1984; Poje, 1985, 1986; Singhvi et al., 1989; Mutić, 1990; Wacha and Frechen, 2011). After the first luminescence dating approach to the sections investigated in this study (Galović et al., 2009), specific investigations were carried out for the Zmajevac loess–paleosol sequences (Molnár et al., 2010; Banak et al., 2012, 2013) and the Šarengrad sequence (Hupuczi et al., 2010; Galović et al., 2011; Wacha et al., 2013). According to Bronger (1976, 2003), at least six paleosols are intercalated in the loess sections from Eastern Croatia, spanning the time period of the Middle and Late Pleistocene (Galović et al., 2009). The later geochemical and/or geochronological investigations of Quaternary aeolian sediments in Croatia were directed to the islands and coastal area of the Adriatic Sea (Wacha et al., 2011; Mikulčić Pavlaković et al., 2011; Pavelić et al., 2011; Romić et al., 2014) and to the Northwestern Croatia (Galović and Peh, 2014; Rubinić et al., 2014, XXXX).

The scope of this work is to investigate the geochemical composition and to correlate those parameters with the sedimentological data of analyzed loess/paleosol sediment successions. Sedimentological data (grain-size coefficients), geochemical content of major, trace and rare earth elements (REE) and acidity (pH), accompanied with previously published data on IRSL dating, grain-size distribution,

* Tel.: +385 1 6160779; fax: +385 1 6144718.
E-mail address: Lidija.Galovic@hgi-cgs.hr

http://dx.doi.org/10.1016/j.aeolia.2014.07.004
1875-9637/

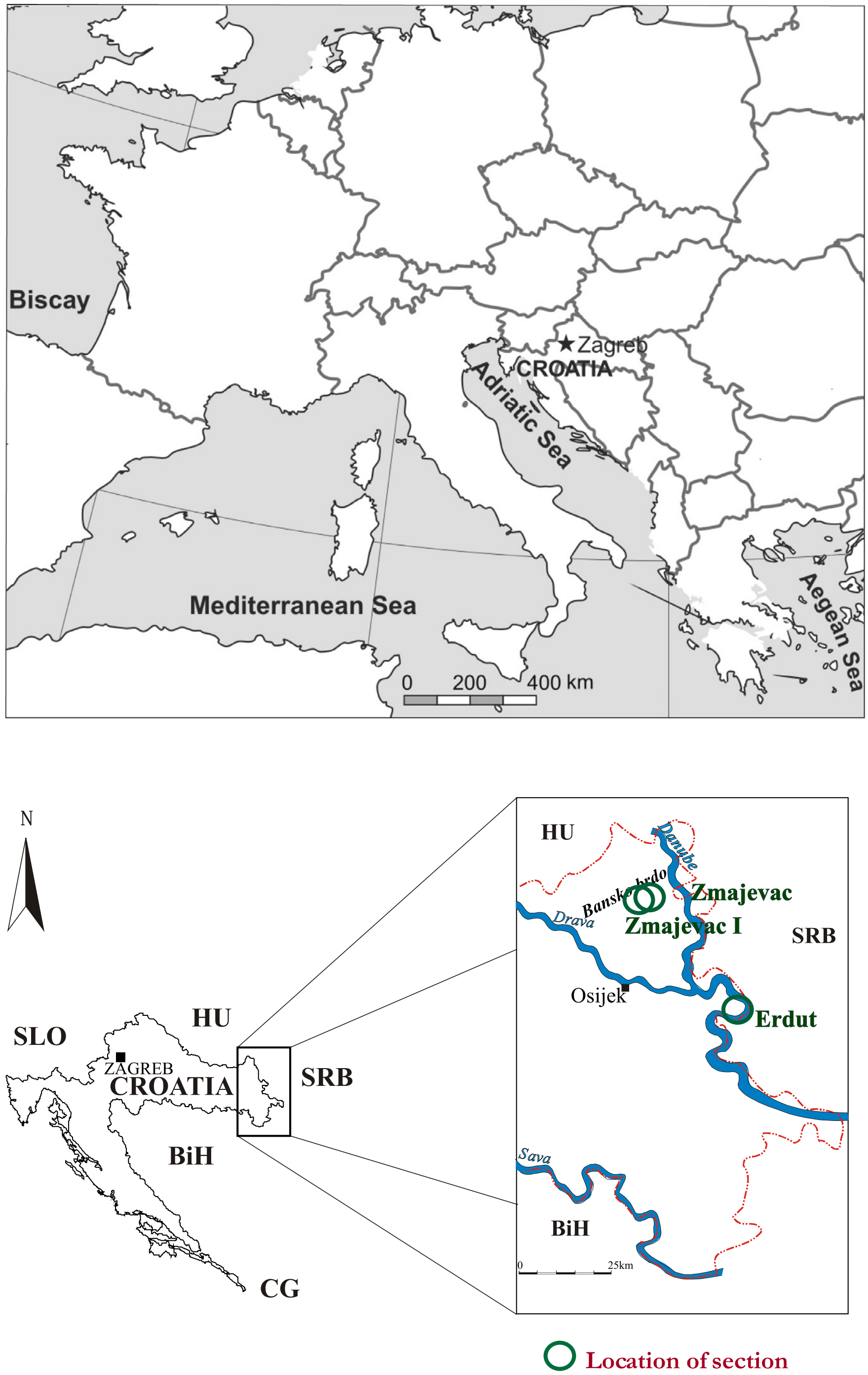

Fig. 1. Map showing positions of sections under investigation in the Eastern Croatia.

organic carbon content (TOC) and $CaCO_3$ content) (Galović et al., 2009) and geochemical and sedimentological characteristics of the Šarengrad section (Galović et al., 2011) highlighted the main characteristics of paleosols and degree of their pedogenesis. Based on these results, another aim of this study is to provide the sedimentological/pedological base for these excellent archives of climate change, entailing environmental change in Croatia. These sequences provide very detailed records of climate change correlating to MIS 2–8, especially if compared with other sections in the Carpathian Basin (Antoine et al., 2009; Bokhorst et al., 2009; Buggle et al., 2008, 2011; Fitzsimmons et al., 2012; Frechen and Pécsi, 2004; Marković et al., 2009, 2011, 2012; Singhvi et al., 1989; Újvári et al., 2014).

2. Geological setting

During the Pleistocene, aeolian sediments were deposited in lakes, pools and shallow marshes in the Croatian Lowland (Bačani et al., 1999) (Fig. 2). Part of these sediments were eroded by the Danube, Drava and Sava Rivers and/or re-deposited downstream as alluvial sediments. Similar deposits were reported and investigated from the Abony section in Hungary (Frechen and Pécsi, 2004).

The Zmajevac I section is described in this publication in detail, while detailed lithostratigraphical subdivisions of the Zmajevac and the Erdut sections are given by Galović et al. (2009).

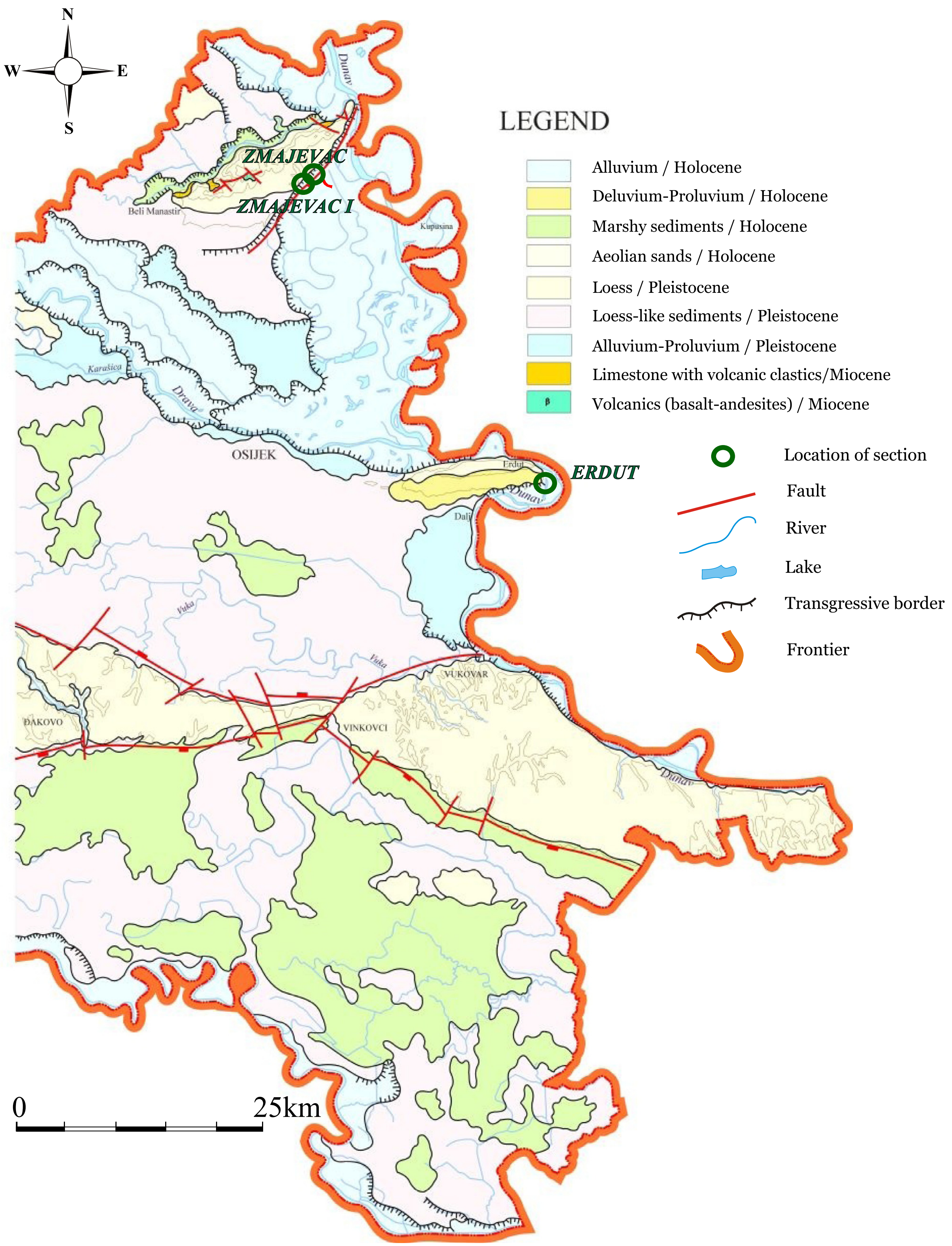

Fig. 2. Geological map of Eastern Croatia (CGS-Department for Geology, 2009) showing positions of the sections.

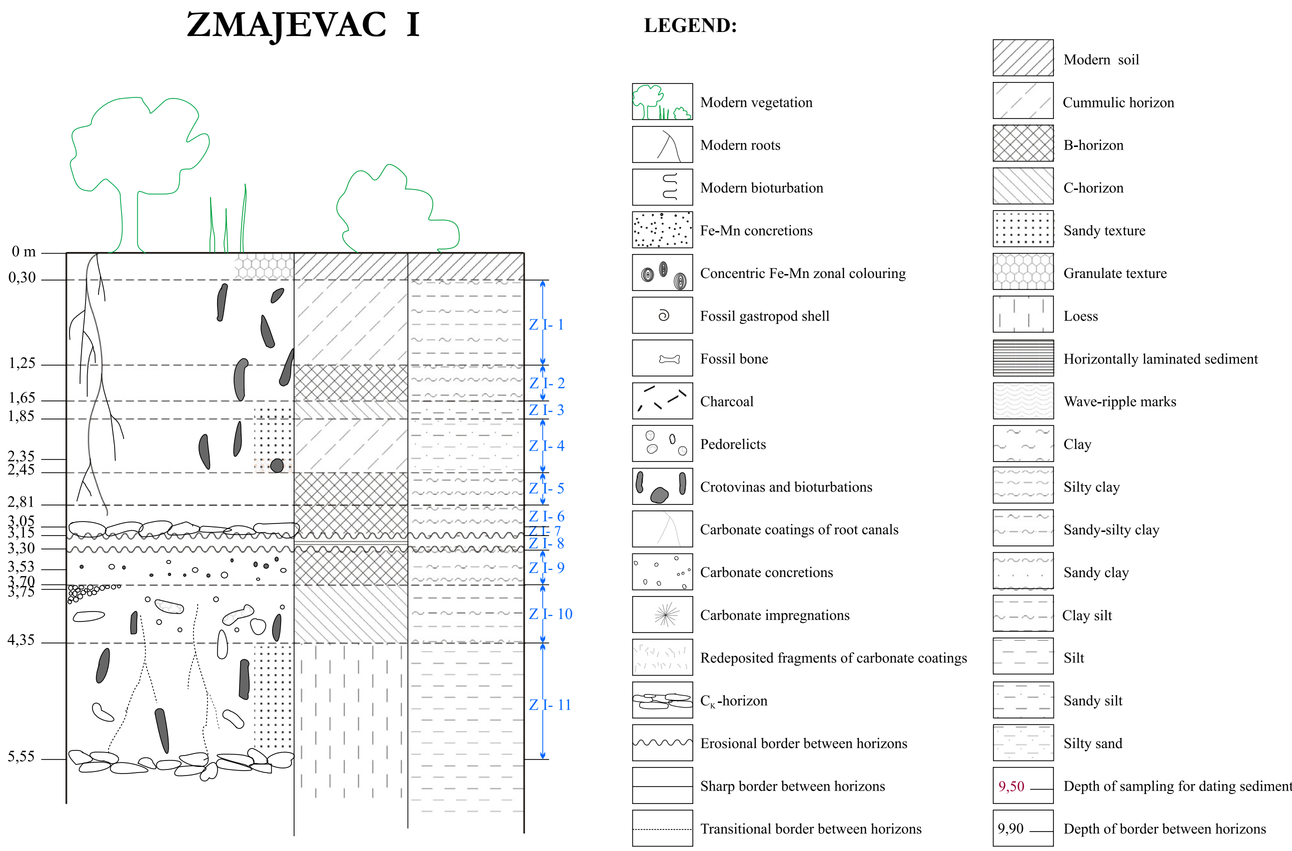

Fig. 3. Field description of the Zmajevac I section.

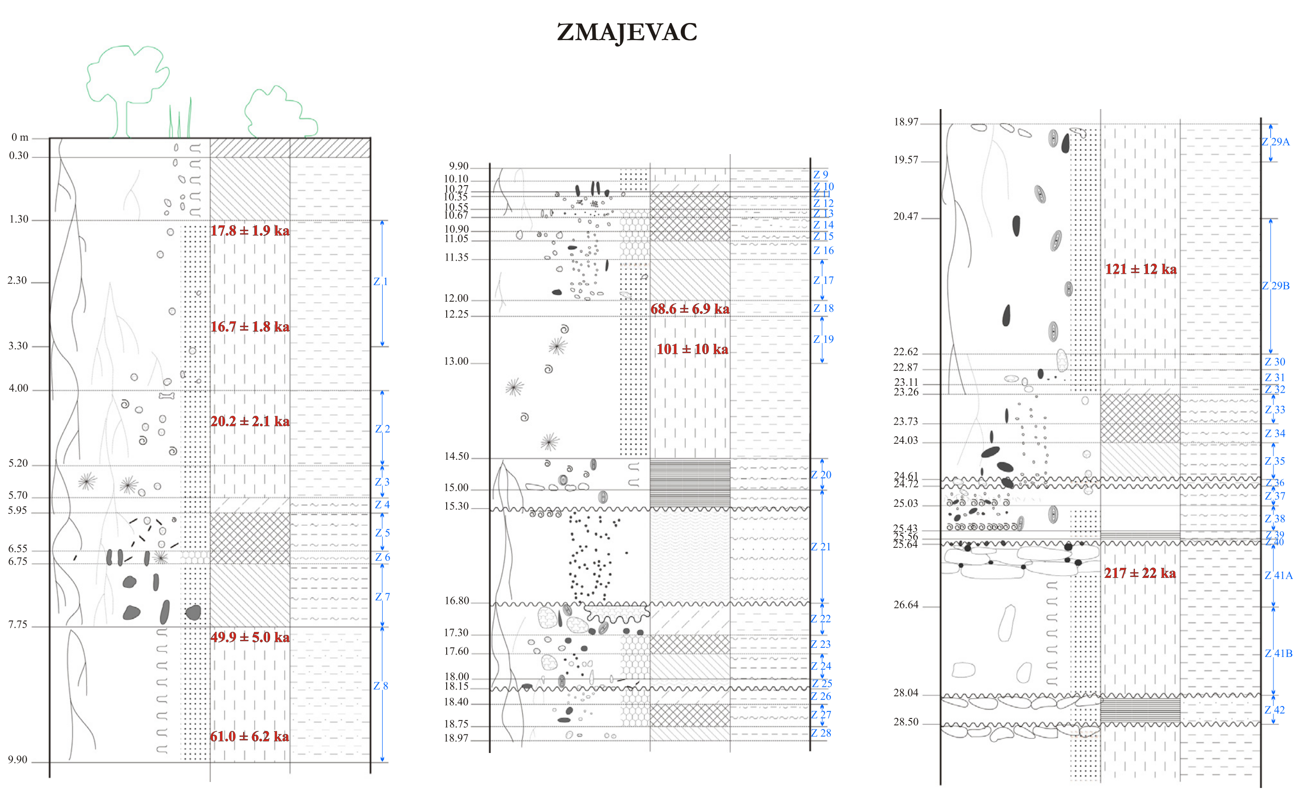

Fig. 4. Field description and luminescence dating results of the Zmajevac section (legend in Fig. 3).

Furthermore, the Šarengrad section has been previously investigated based on both, the geochronology and geochemistry, and its geological setting is described in detail (Galović et al., 2009, 2011).

2.1. Zmajevac

The Bansko Brdo is an asymmetric tectonic horst elongated NE-SW with elevation of about 243 m above sea level (asl.) which is the highest in the study area. Tectonic activity caused synsedimentary effusion of basalto-andesite and deposition of volcanic breccias. The Miocene age of andesites is confirmed by K-Ar dating (14.5 ± 0.4 and 13.8 ± 0.4 Ma at two locations) (Pamić and Pikija, 1987). The loess is exposed on top of the volcano-clastic material. More recent, tectonic uplift formed a complex horst – the Bansko Brdo. Loess–paleosol sequences are exposed along its south-eastern slope. These neotectonic movements are still active (Galović et al., 2009) (Fig. 2).

2.1.1. Zmajevac I section

The Zmajevac I section (45°48′37″ N. Lat., 18°49′02″ E. Long.) is about one kilometre to the NE from the centre of Zmajevac. The elevation is about 95 m asl. (Fig. 1). The sediment succession has a total thickness between 6 and 8 m, and only 5.5 m of the bottom part that was reachable was studied. Throughout the sequence, the three paleosols are intercalated in the loess (Fig. 3).

At the bottom of the investigated profile is silty light yellowish brown (2.5 Y 6/3) (Munsell Soil Color Charts, 2000) carbonate loess sediment. Carbonate concretions 5–10 cm in diameter form Ck-horizon. They are precipitated at the contact between lower loess and 80 cm thick light yellowish brown (2.5 Y 6/4) silty C horizon (ZI-11) of the well-developed upper soil. Grain-size fines upward with increase of number of crotovinas. Crotovina is animal burrow that has been filled with organic and/or mineral material from another horizon (Retallack, 2001). Along a light yellowish brown (10 YR 6/4) 65 cm thick transitional carbonate BC-horizon (ZI-10), grain-size fines upward from silt to clay silt. Quantity of crotovinas is increasing upward (up to 15 cm in diameter), and their content is intensively bioturbated silty clay, ranging in colour from reddish brown to yellowish red (5 YR 4/4–4/6), originating from the upper B-horizon (ZI-9). Root channels are filled with red (2.5 YR 5/6) silt. Rare spherical carbonate concretions (5–10 cm) and vertical and sub-vertical root channels are surrounded by concentric reddish-yellow iron-oxide staining zones, formed around root channels. In the upper 15 cm of horizon, a lens-shaped accumulation of redeposited carbonate concretions (up to 1 cm in diameter) inclines laterally and indicates truncated erosional upper boundary of the horizon. The hydromorphic Bg-horizon (ZI-9) is presented by 40 cm thick yellowish red (5 YR 4/6) massive silty clay, postpedogenetically exposed to ground water, with Fe/Mn-concretions up to 2 mm in diameter.

Stratigraphically the oldest exposed hydromorphic paleosol is covered by 2–15 cm thick, carbonate rich, laminated alluvial sediments and loess (ZI-8). This horizon contains laminas two to three cm thick. Redeposited material is composed of a reddish brown (5 YR 4/4) eroded ZI-9 horizon, most probably from a local hypsometrically higher position, and olive yellow (2.5 Y 6/6) loess, deposited during dry period. Bioturbation of laminas indicates postsedimentary pedogenesis. The upper erosional boundary is covered by 10 cm thick accumulation of carbonate concretions, crushed carbonate coatings and fossil remains of bones and gastropod shells (ZI-7).

The second paleosol is a brown soil, about 1.2 m thick, comprised of two horizons: gleyic yellowish brown (10 YR 5/6) Bg-horizon consists of 24 cm thick ZI-6 and 36 cm thick ZI-5 layer. Carbonate is present only in the form of coating of soil granules (pseudo-mycelium) in the bottom part of ZI-6 horizon. The cumulic horizon ZI-4 is light yellowish brown (2.5 Y 6/3), 60 cm thick, carbonate-free, with sporadic crotovinas filled with lighter dryer olive yellow (2.5 Y 6/6) silt.

The uppermost paleosol (ZI-3–ZI-1) is weakly developed carbonate free 1.55 cm thick paleosol, which is superimposed by 30 cm of modern soil activity at the top of the investigated sequence. ZI-3 is 20 cm thick light olive brown (2.5 Y 5/3) silty BC-horizon. Horizon ZI-2 is 40 cm thick (10 YR 4/3) clay silt slightly altered by recent pedogenesis. This B-horizon contains rare vertical and sub-vertical crotovinas, filled with light gray (2.5 Y 7/2) silt, materials which are absent in the overlying sediments, indicating eroded younger sediments. Overlaying 95 cm of the cumulic horizon (ZI-1) is light olive brown (2.5 Y 5/4) silt. The filling of vertical and subvertical crotovinas is same as in ZI-2 horizon: light gray (2.5 Y 7/2) silt.

2.1.2. Zmajevac section

The investigated section is situated 45°48′49″ N. Lat. and 18°49′33″ E. Long., at an elevation of 90 m asl., about 2 km to the NE of the village of Zmajevac and about 1 km away from the Zmajevac I section. The sediment succession has a thickness of 28.5 m. Four paleosols, six loess layers and alluvial sediment can be distinguished (Fig. 4).

The stratigraphically lowest sediment of the sequence consists of silty loess more than 200 cm thick. On the top of that loess layer, carbonate is enriched, forming a solid, about 10 cm thick, Ck-horizon. It almost completely consists of homogenous horizontally to sub-horizontally layered platy carbonate concretions up to 50 cm in diameter, indicating oscillation of water table. Above that layer, about 45 cm thick loess (Z-42) is deposited and another platy carbonate layer is formed in the upper 10 cm of this horizon.

The upper Ck-horizon is covered by silty loess (Z-41A–Z-41B) about 240 cm thick, yielded an IRSL age estimate of 217 ± 22 ka (OIS 8), containing many modern insect holes, indicating a sandier composition. Smaller carbonate concretions are up to 15 cm in diameter, and their size is increasing upward up to 50 cm in diameter. The upper boundary is truncated and covered by accumulations of gastropod detritus and carbonate-rich material in lens-like structures.

This horizon is covered by a well-developed brown pedocomplex about 275 cm thick, intercalated by several erosional discontinuities. This is soil-sediment that was exposed to pedogenetic development after redeposition of the soil. It contains several zones enriched in redeposited carbonate fragments or laminated sediment. The pedocomplex is comprised of 161 cm thick basal BCk-horizon (Z-40–Z-35), overlain by 77 cm thick B-horizon (Z-34–Z-33), topped by 40 cm thick cumulic horizon (Z-32–Z-31).

Above the pedocomplex is 390 cm thick silty loess (Z-30–Z-29A), with an IRSL age estimate of 121 ± 12 ka (OIS 6), covered by another pedocomplex about 220 cm thick. The lower brown paleosol (Z-28–Z-26) is pedosediment and consists of BCk-horizon 22 cm thick, a 35 cm thick B-horizon, and a 25 cm thick cumulic horizon. The upper brown soil (Z-24–Z-22) overlies the pedosediment (Z-28–Z-26). These two paleosols are intercalated by up to 15 cm thick laminated sediment (Z-25) which laterally increases in thickness. Furthermore, each paleosol is truncated and covered by laminated sediments. The upper laminated sediments (Z-21–Z-20) have a thickness of 230 cm, and continuously extend laterally across the outcrop. There is a sharp discontinuity between horizon Z-21, characterized by ripple marks and Fe/Mn-rich nodules, and the horizontal laminated horizon Z-20, which indicates a low-energy sedimentary environment.

These horizons are covered by silty loess (Z-19–Z-18) about 250 cm thick. Two samples taken from the loess yielded IRSL age estimates of 101 ± 10 and 68.6 ± 6.9 ka. A well-developed brown paleosol (OIS 5) about 190 cm thick is exposed above the loess.

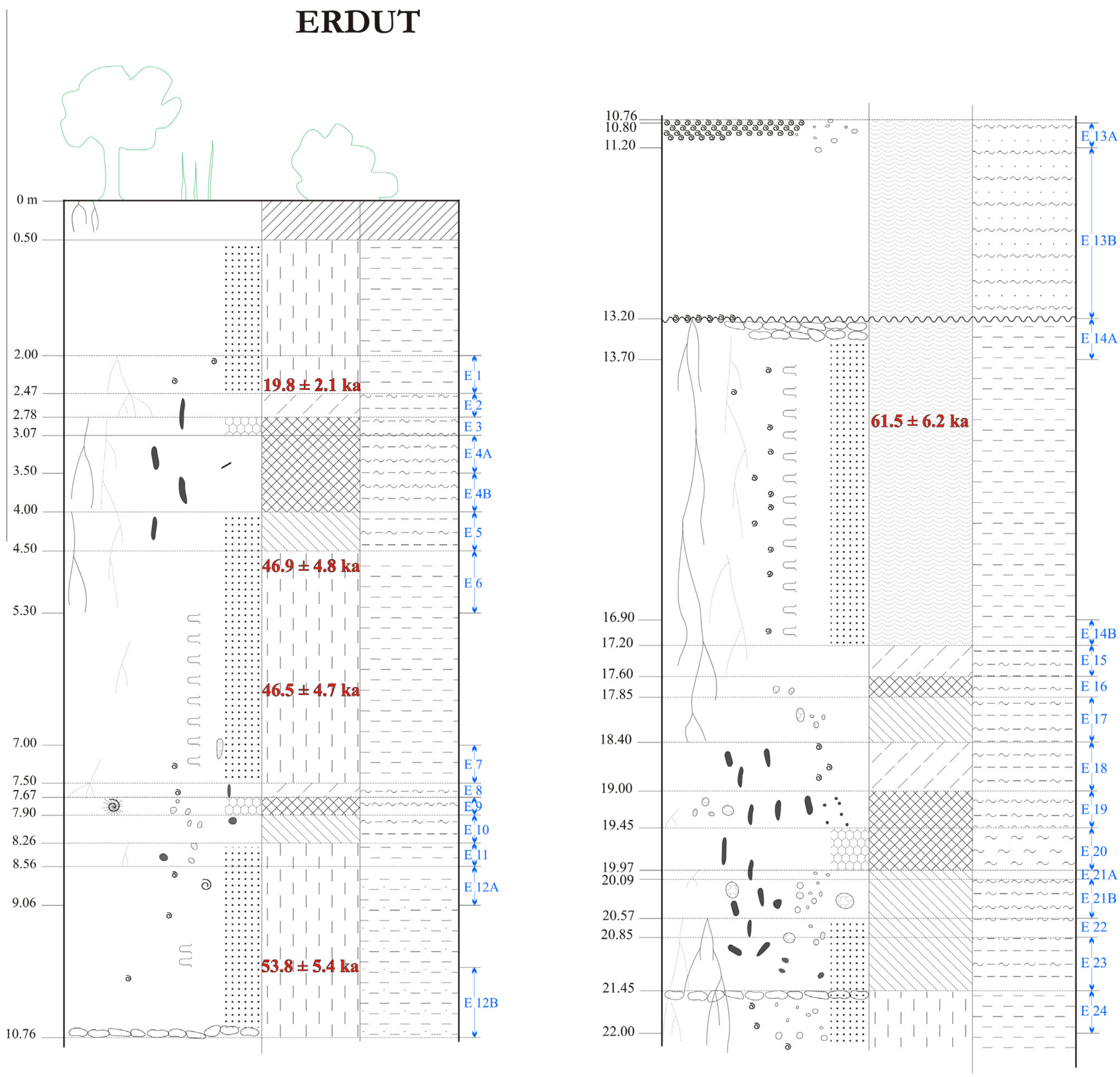

Fig. 5. Field description and luminescence dating results of the Erdut section (legend in Fig. 3).

The lower part (Z-17–Z-16) designated as a BCk-horizon, is 95 cm thick. Carbonate content increases with depth. The Bt-horizon (Z-15–Z-11) is bioturbated. The cumulic horizon (Z-10) is 17 cm thick, with crotovinas filled with material from the underlying sediment.

The loess layer (Z-9–Z-8) is 235 cm thick. A weakly developed yellowish brown paleosol about 205 cm thick overlies the loess. This paleosol (OIS 3) consists of 100 cm thick BCk-horizon (Z-7) intermingled by crotovinas. The B-horizon (Z-6–Z-5) is 80 cm thick and has soft pieces of charcoal and many bioturbation features. A cumulic horizon (Z-4) has a thickness of 25 cm.

This paleosol is covered by 440 cm thick silty loess with many gastropod shells (Z-3–Z-1) and overlain by a modern rendzina soil at the top of the section. The stratigraphically youngest loess gave IRSL age estimates ranging from 16.7 ± 1.8 to 20.2 ± 2.1 ka (OIS 3), indicating a period of increased accumulation of aeolian dust during the last pleniglacial/late glacial.

2.1.3. Erdut section

The bedrock of the horst of the Erdutsko Brdo consists of Miocene conglomerates, limestones and sandstones, covered with lower Pliocene clayey and sandy sediments (Galović et al., 2009). At the beginning of the Quaternary, the subsidence rate increased resulting in intensive sedimentation. Tectonic activity during the Middle and Upper Pleistocene caused the uplift of the Erdutsko Brdo, whereas the northern and southern slopes relatively subsided (Bačani et al., 1999). The northern fault has been reactivated more recently, resulting in steep exposures of loess–paleosol sequences along the northern slope of the Erdutsko Brdo.

The Erdut section (45°30′49″ N. Lat., 19°04′57″ E. Long.) is located in front of the bridge crossing the Danube River near the village of Erdut, at an elevation of about 100 m asl. The sediment succession has a thickness of about 22 m. At least four paleosols, five loess layers and alluvial sediments are distinguished (Fig. 5).

At the bottom of the investigated profile, loess is exposed and covered by relatively homogenous silty loess about 45 cm thick, designated as a Ck-horizon, with few carbonate concretions. Large carbonate concretions up to 20 cm in diameter occur at the contact between the well-developed brown to strong brown soil (E-23–E-18) and the underlying loess (E-24). The average thickness of the overlying pedocomplex is 305 cm, and includes several soil horizons of different pedogenic intensity and colour. The basal BC-horizon (E-23–E-21A) is about 148 cm thick, characterized by crotovinas and carbonate coatings. The carbonate content increases with depth. The B-horizon (E-19–E-20) is about 97 cm thick and has a diffuse transition upward to the overlying cumulic horizon (E-18).

This strongly developed pedocomplex is covered by a 120 cm thick light yellowish brown soil with weak humification and consists of a 25 cm thick BC-horizon (E-17), a 55 cm thick bioturbated B-horizon (E-16) and a 40 cm thick cumulic horizon (E-15).

The loess layer (E-15–E-14A), with many gastropod shells and modern insect holes, has a thickness of 400 cm and gave an IRSL age estimate of 61.5 ± 6.2 ka. The upper part of the loess is truncated and covered by laminated alluvial sediments, probably deposited by the "Paleo-Danube". The alluvial sediments (E-13B–E-13A) have a thickness of about 250 cm and consist of approximately 40 sets of laminas, characterised by ripple marks, slumping, and fining upward cycles, mainly composed of redeposited loess material. The upper boundary of the laminated sediments is covered by a horizon of broken gastropod shells and secondary carbonate concretions in small lenses.

Loess covering the alluvial sediments is sandy silt, has a thickness of 250 cm (E-12B–E-11) and yielded anIRSL age estimate of 53.8 ± 5.4 ka. The loess is covered by a 76 cm thick weakly developed yellowish brown paleosol with vertical and sub-vertical crotovinas. The paleosol consists of a 36 cm thick BC-horizon (E-10), a 23 cm thick B-horizon (E-9) and a 17 cm thick cumulic horizon (E-8).

This paleosol is covered by 300 cm thick porous loess. The upper 200 cm of this layer consists of carbonate-free loess (E-6; IRSL age estimates of 46.5 ± 4.7 ka), while the remaining part of the loess layer (E-7; IRSL age estimates of 46.9 ± 4.8 ka) and all the older sediments in this loess–paleosol sequence are calcareous. The carbonate-free loess is about 200 cm thick and is superimposed by a dark yellowish brown paleosol (E-5–E-2). The lowermost 50 cm (E-5) of the paleosol is the BC-horizon. The thickness of the overlying B-horizon is about 122 cm. It includes clay horizons (E-4A–E-4B) containing charcoal and E-3. At the top of this paleosol, 31 cm of cumulic silty horizon (E-2) is exposed. Those paleosol horizons are heavily bioturbated. The carbonate content of the paleosol decreases with depth. An IRSL age estimate of 19.8 ± 2.1 ka was determined for the stratigraphically youngest carbonate-rich silty loess layer (E-1). Its thickness varies from 200 to 500 cm, depending on the modern relief. An A horizon about 50 cm thick forms the modern soil.

3. Sampling and methods

Eighty-two samples were collected from the Zmajevac I, Zmajevac and the Erdut sections (including loess, paleosols and alluvial sediments) for sedimentological (grain-size) and geochemical investigations. The measured values for investigated paleosols served to explain the main characteristics and degree of pedogenesis.

Samples were air-dried at temperature <40 °C for approximately 1 month in order to prevent the loss of volatile components and sieved to the <2 mm fraction to separate the sediment from larger carbonate concretions, while smaller, if present, remained in the samples.

The laboratory investigations of 10 samples from the Zmajevac I section included grain-size analysis (sieving and aerometry), measuring pH, determination of carbonate content, determination of TOC and geochemical analysis of major and trace elements and REE. Samples from the Zmajevac and the Erdut sections ($n = 82$) were analyzed only for their geochemical composition and acidity, since the results of the other aforementioned analyses were published in Galović et al. (2009), wherein those methods have been reported in detail.

3.1. Grain-size analyses

Grain-size analysis was performed by sieving (1.25 mm; 0.9 mm; 0.45 mm; 0.25 mm; 0.125 mm and 0.09 mm size-fractions) using pipette method, followed by removal of soil organic matter with H_2O_2, carbonates with 4% HCl and dispersion with Na_2SiO_3 (HRN ISO 11277:2004), as described in Galović et al. (2009). Particle sizes between 2 and 0.06 mm are defined as sand, between 0.06 and 0.004 mm as silt, and smaller grains as clay particles. Median (Md), sorting coefficient (S_o) and skewness (S_k) were calculated in order to determine their specific distribution in soil profiles (Folk, 1974).

3.2. Geochemical analysis

Air-dried samples were sieved to the <0.125 mm fraction. This fraction was used following some earlier investigations showing that high content of most elements, particularly the trace elements, is present in the fine-grained fraction (Darnley et al., 1995; Salminen et al., 1998, 2005; Miko et al., 2001; Galović et al., 2011; Halamić et al., 2003; Peh et al., 2008; Šajn et al., 2008). In addition, this fraction usually contributes to more than 95% of the particles in most loess, paleosol and related alluvial sediment samples. Oreščanin et al. (2005) concluded that in recent channel sediments of the Danube River in the village of Batina, the greatest proportion of the total heavy metal load is contained in the clay and silt fraction.

3.2.1. Acidity, carbonate content and TOC

Acidity was measured in a 1:5 soil/water ratio, following Van Lagen procedure (1993), using MettlerToledo MPC 227 pH-meter in the Laboratory for soil analyses, Faculty of Agriculture, Zagreb.

Carbonate content was analyzed by gas volumetry, measuring the volume of CO_2 (Van Lagen, 1993) after reaction with HCl (c (HCl = 4 mol L^{-1})) using Scheibler-instrument (HRN ISO 10693:2004).

Total organic carbon (TOC) was measured using LECO C IR-212 with microprocessor by the method developed at Robertson Research International Ltd. Samples were decarbonised by adding diluted HCl (1:1) and slightly heated and dried. Then the samples were burned at a temperature ranging from 1100 to 1300 °C.

3.2.2. Major, trace and REE elements

A bulk of 0.25 g of dry material per sample was homogenized in agate mortar and was, after the near total decomposition (a hot acid mixture of $HClO_4$–HNO_3–HCl–HF at 200°C), analyzed for the set of 41 major and trace elements by inductively-coupled plasma mass spectrometry (ICP-MS) at the ACME Analytical Laboratories in Vancouver (Canada). The following elements were analyzed: Ag, Al, As, Au, Ba, Be, Bi, Ca, Ce, Cd, Co, Cr, Cs, Cu, Dy, Er, Eu, Fe, Ga, Gd, Hf, Ho, K, La, Li, Lu, Mg, Mn, Mo, Na, Nb, Nd, Ni, P, Pb, Pr, Rb, S, Sb, Sc, Sm, Sn, Sr, Ta, Tb, Th, Ti, Tm, U, V, W, Y, Yb, Zn, and Zr. The digestion was only partial for some Cr and Ba minerals and some Al, Fe, Hf, Mn, Sn, Ta and Zr oxides. The volatilization during fuming may have also resulted in some loss of As, Sb and Au, while Si was completely volatilized by HF.

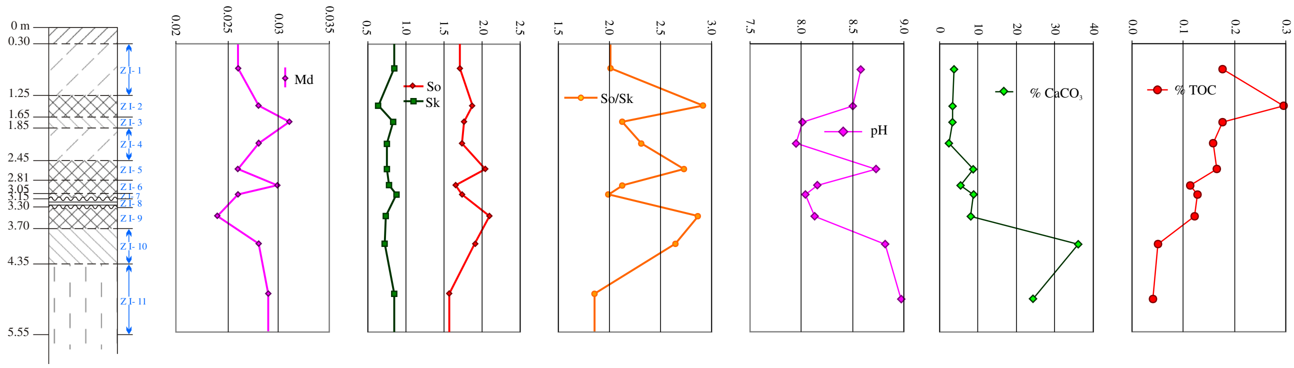

Fig. 6. Grain-size coefficients (Md, S_o, S_k), their ratio, acidity, carbonate content and TOC content of the Zmajevac I section. Md, median; S_o, sorting coefficient; S_k, skewness.

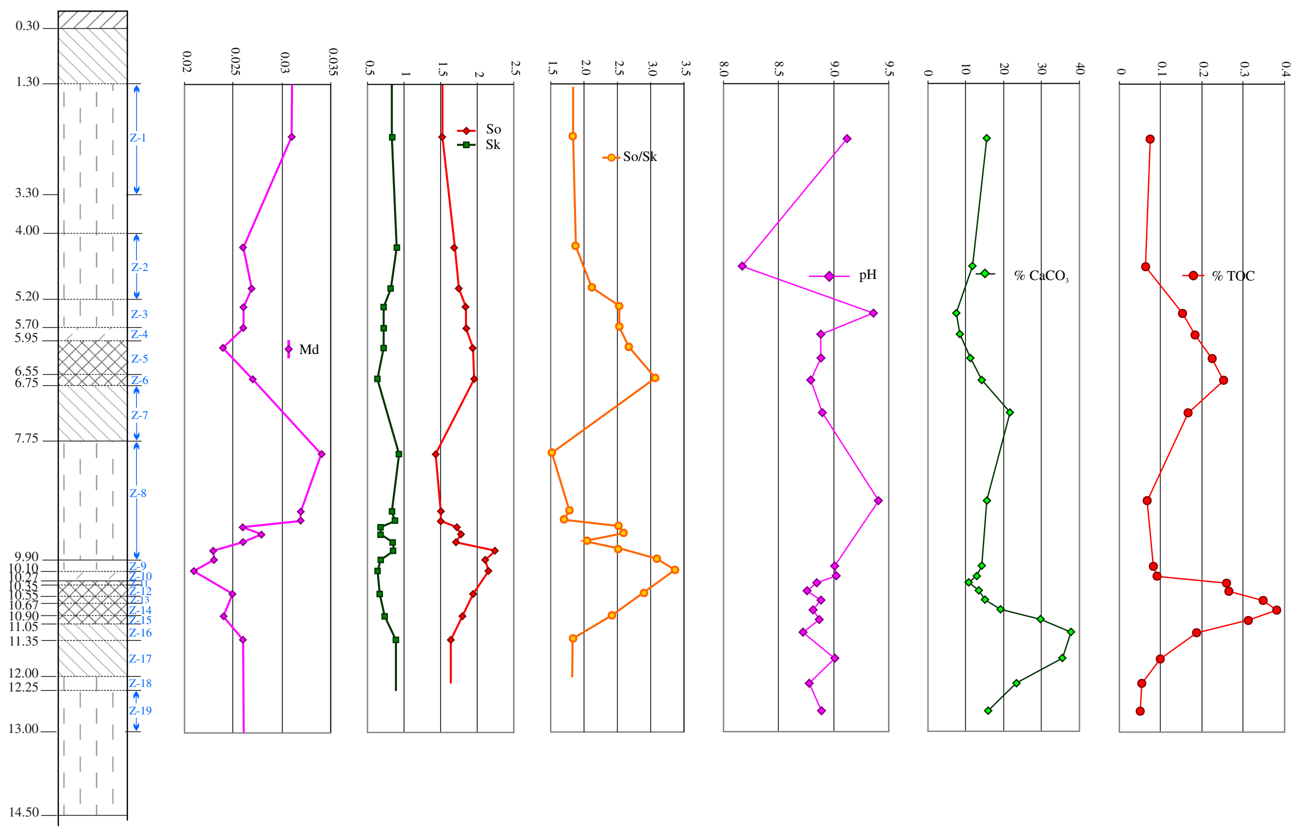

Fig. 7. Grain-size coefficients (Md, S_o, S_k), their ratio, acidity, carbonate content and TOC content of the Zmajevac section. Md, median; S_o, sorting coefficient; S_k, skewness.

All samples ($n = 82$), their duplicates ($n = 12$) and geologic standards ($n = 5$) were submitted to the laboratory in a random order. This procedure assured unbiased treatment of the samples and random distribution of the possible drift of analytical conditions for all samples. The resulting coefficient of variation is, on average, approximately 5%, with exception of Ag with measurement precision of 13% and of Cd 10% (Galović et al., 2011). The accuracy of the analyses was additionally controlled by certified geological reference materials (DST5, ACME Laboratory; $n = 5$). The analytical results for Au, S, Be and Ta were excluded, because more than 50% of the samples contained concentrations below the instrumental detection limits, or their accuracy and/or precision were out of range of ±10% of the certified values (Peh et al., 2008; Galović et al., 2011; Halamić et al., 2012; Šajn et al., 2011). Percentages of major elements were converted to oxide weight percents. These data could not be normalized to their molecular weight owing to insufficient number of data points. Analytical results of trace elements and REE are presented as mg kg^{-1}.

3.3. Weathering coefficients

The concept of geochemical proxies of mineral alteration (i.e., weathering coefficients) relies on the selective removal of soluble and mobile elements from a weathering profile compared to the relative enrichment of rather immobile and non-soluble elements. To approximate pedogenetic processes (Retallack, 2001), weathering coefficients were determined to estimate the base loss [$(CaO+Na_2O+MgO+K_2O)/Al_2O_3$], the leaching (Ba/Sr), the degree of feldspar weathering [$(Na_2O+K_2O)/Al_2O_3$] and the ratio of plagioclase and K-feldspar weathering (Na_2O/K_2O) (Buggle et al., 2008, 2011; Bokhorst et al., 2009; Kahmann and Driese, 2008; Bogucky et al., 2009; Galović et al., 2011; Újvári et al., 2014).

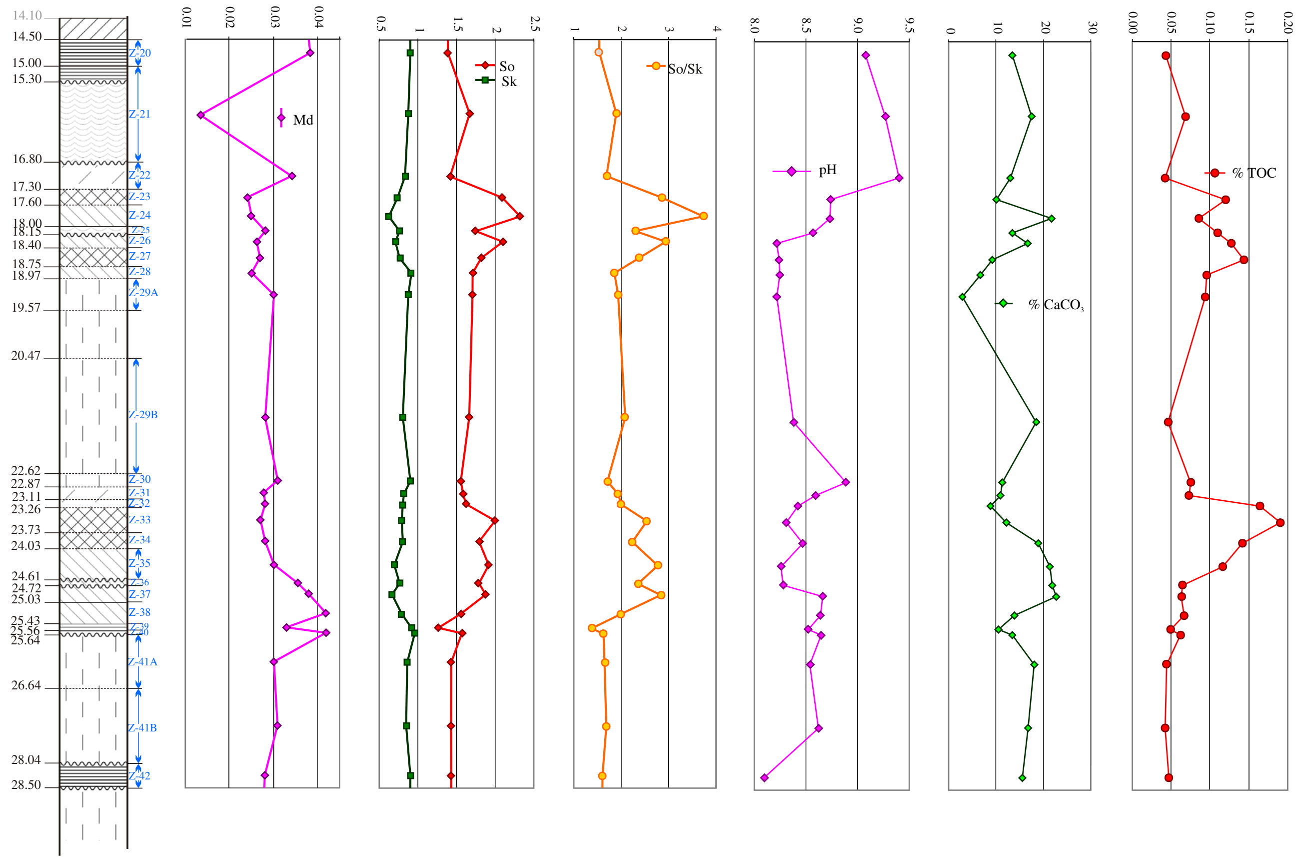

Fig. 7 (*continued*)

4. Results and discussion

4.1. Grain-size analyses

The granulometric compositions of the Zmajevac and the Erdut sections are presented in Galović et al. (2009). Silt is the dominant grain-size fraction in the sediments under the study. In about 90% of analyzed horizons, there is equal share of small-, medium- and coarse-grained silt. Exceptions are alluvial sediments with dominating finer (Z-21) or coarser (E-13A) fractions and cumulic E-15 horizon. Generally, sand fraction is represented by a larger portion than clay fraction, except in the upper parts of paleosols, especially in the older parts of the sections, where pedogenetic processes were the most intensive (Galović et al., 2009).

In the Zmajevac I section, the sorting coefficients (S_o) are medium to very low and they increase in paleosol horizons. Since the skewnesses (S_k) in the same horizons decreases, the ratio of these two coefficients clearly distinguishes the paleosol horizons from the loess horizons. In the paleosol horizons the ratios S_o/S_k are >2.2 (Fig. 6).

The medians (Md) of the Zmajevac section oscillate noticeably. They are >0.03 in the horizons macroscopically characterized by drilling of organisms (see Section 2). The S_o and S_k coefficients have almost symmetrical and reciprocal diagrams. They clearly mark the sampled paleosols so that, based on the assumed limit of 2.2 for the S_o/S_k ratios, single paleosols within the three older pedocomplexes could be distinguished (Fig. 7).

In the sample E-15 from the Erdut section, the percentage of coarse silt fraction is extremely high (>80%). The grain-size composition has been confirmed after multiple repeated analyzes. Md coefficient in the loess samples is about 0.03, and around 0.025 in the paleosol samples (Fig. 8). The median has maximum value in laminated horizons, characterized by recent drilling (burrow and nesting). Based on the S_o/S_k ratios, four paleosols (two paleosols and a pedocomplex) can be clearly extracted. Furthermore, for each paleosol, the degree of pedogenetic development can be realized.

4.2. Acidity

The acidity measured in these samples was unstable even after 2 h of soaking (see Section 3.2.1). Namely, calcium carbonate was still solving, thereby changing pH of the suspensions of the samples and water continuously. Therefore, the pH values of the suspensions were measured after 2.5 h of soaking, in order to achieve the same conditions for all samples.

Acidity changes during postpedogenetic processes. The pH of the samples is analyzed usually within the range of values between 8 and 9, indicating slightly basic conditions (Figs. 6–8). If acidity of individual paleosols along the sections is observed separately, it is noted that the older paleosol of the Zmajevac I, Zmajevac and Erdut sections have higher acidity than the younger paleosols. The exception is the Zmajevac I section, where this trend is not observed because of shortness of the section, rendering determination of a general trend more difficult.

In horizons with higher pH values (Figs. 6–8), carbonates are more frequent and in various forms (loess dolls, incrustations of roots, rhizoconcretions, carbonate coatings of soil aggregates, hypo-coatings and coatings). Leaking of an aqueous solution of carbonate through the loess section leads to increase of pH and carbonate precipitation. At the same time, the precipitation is changing acidity of horizons. This explains processes during pedogenesis and immediately afterwards.

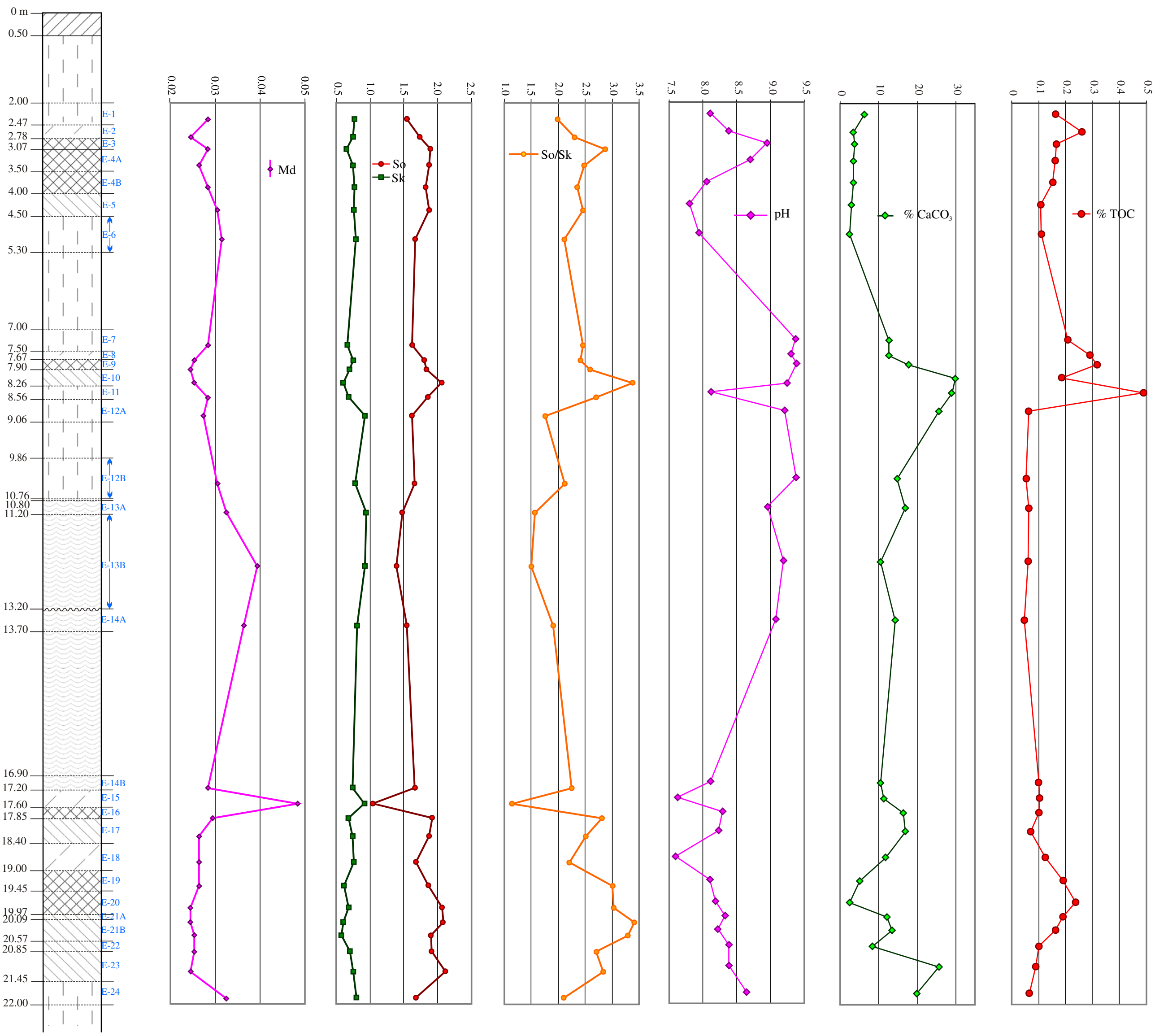

Fig. 8. Grain-size coefficients (Md, S_o, S_k), their ratio, acidity, carbonate content and TOC content of the Erdut section. Md, median; S_o, sorting coefficient; S_k, skewness.

4.3. Carbonate content

The distributions of carbonate along the analyzed profiles (Figs. 6–8) suggest the trend of increasing carbonate content with an increase of depth. Furthermore, within each paleosol (with the exception of the youngest non-carbonate part of the sections Zmajevac I and Erdut; Figs. 6 and 7), there is an increase of carbonate content with depth up to almost 40% of carbonate fraction (recalculated on calcium carbonate) (see Fig. 7: Z-16 and Z-17).

4.4. TOC analysis

Total organic matter (measured by analyzing the total organic carbon – TOC) is one of the best indicators of the degree of pedogenetic development. In the loess horizons TOC is <0.1%, while, in paleosol horizons, it is between 0.1% and 0.5%. In most cumulic horizons, TOC values are slightly lower than in referred paleosols. Thus, in well-developed paleosols, the portion of TOC is increasing toward B-horizons, and then reducing toward C-horizons. Older paleosols have a lower content of organic carbon than the younger paleosols (Figs. 6–8). This is probably due to postdiagenetic changes caused by compaction of sediments and oxidation.

4.5. Geochemical analysis

The contents of major, trace and REE were measured for 82 samples. The analytical results are shown in Figs. 9–11. Distributions of analyzed elements are normal, with exception of Ca, Mg and Sr, because of big number of carbonate-free horizons. Elementary statistics for concentrations of all analyzed elements indicates that there is no significant difference in chemical composition among studied sections, because they are all composed of composite of paleosol, loess and laminated sediments.

The reliability (precision, accuracy and detection limits) of analytical method is presented in the Section 3.2.2.

4.5.1. Major elements

The vertical distributions of TiO_2, Al_2O_3, Fe_2O_3, K_2O, MnO, NaO and P_2O_5 are almost parallel (Figs. 9–11). Generally, the trend is enrichment of those major elements in cumulic horizons, resulting in a maximum value in the upper part of B-horizons, but decreasing

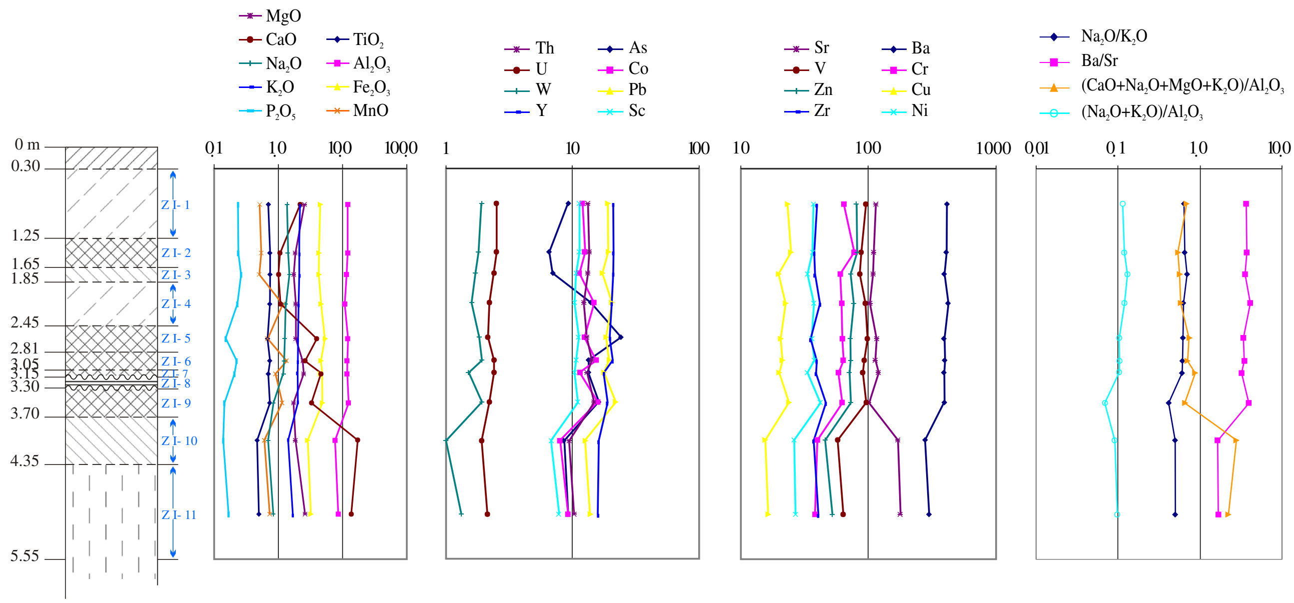

Fig. 9. Distribution of concentrations of major elements (without SiO_2 and LOI) (values in wt.%), trace elements (values in mg kg^{-1}) and weathering coefficients of the Zmajevac I section; as measured by ICP-MS.

in BC-horizon. Enrichment with major elements responds to the degree of pedogenetic development. The distributions of CaO and MgO are opposite to distribution of oxides of other major elements (Figs. 9–11), concentrating in C-horizons in secondary carbonates.

4.5.2. Trace elements

Trace elements are characterized by a few typical vertical distributions in accordance to depth (Figs. 9–11).

The analyzed concentrations of trace metals, like Cu, Cr, W, Y, Nb, Sn, Pb, Bi, Li, Ni, Rb, Zn, V, Ga, Ba and Sb, have similar distribution along the investigated profile, but their concentrations and ranges of concentrations are different. Their vertical distribution curves are almost identical, but shifted along abscissa (Figs. 9–11). Their concentrations generally increase with profile depth and reach local maximums in each B-horizon. They are more abundant in cumulic and B-horizons than in BC- and loess horizons. Their presence is the function of pedogenesis and increases with the degree of pedogenetic development. In each analyzed section, the uppermost paleosols are enriched with those elements, and the highest concentrations are in older paleosol horizons. Exception is as distribution in upper part of the Zmajevac I section (Fig. 9). Uranium and zirconium (low mobile elements) follow the trend, but not as distinctly as wolfram and cooper (mobile elements). Zircon is the main mineral of Zr and is extremely resistant to weathering. Thus, the content of Zr in analyzed horizons does not reflect exposure to pedogenetic processes.

Specific distribution of Sr concentrations follow the distribution of Ca because of their isomorphic exchange in carbonates (see Section 4.5.1).

4.5.3. Weathering coefficients

$(CaO+Na_2O+MgO+K_2O)/Al_2O_3$ is a coefficient that yields qualitative information about the loss of bases. The coefficient decreases with depth and varies significantly, so the measured values range from 0.4 to 3.5, but the most of the value is within the limits of 0.7 and 1.6. Each B-horizon is a local minimum. The lowest values are in the most developed paleosol horizons of analyzed sections and in the youngest paleosol of the Erdut sections that was developed on non-carbonate loess (Figs. 9–11).

Coefficient Ba/Sr is the leaching coefficient that represents resistance to drainage (estimation of leaching). It is commonly used to reflect the chemical weathering intensity, due to the solution rate diversity between Sr and Ba during the pedogenic processes (Liang et al., 2013). Ba is resistant element with lower mobility, and Sr is very mobile in pedogenetic environment. The distribution of Ba/Sr is nearly a mirror image of base loss distribution $(CaO+Na_2O+MgO+K_2O)/Al_2O_3$. It is up to 4.5 times higher in paleosols than in loess or BC-horizons, respectively, which is a consequence of the reduced strontium in paleosols (leaching) (Figs. 9–11).

The Na_2O/K_2O weathering coefficient shows ratio of plagioclase and K-feldspar. Based on homogenous mineral composition (Banak et al., 2013; Wacha et al., 2013), lower ratio indicates intense weathering of les resistant plagioclase and higher degree of pedogenesis. It is higher in loess than in paleosols, owing to a higher content of K in clay fraction and leaching of Na. In each paleosol, the ratio decreases from cumulic horizon to B-horizon, but slightly increases in the BC-horizon. Generally, this coefficient decreases with depth. The lowest values were registered in the redeposited loess/paleosol material (Z-21), the soil sediment from the bottom of the Zmajevac I section (ZI-9–ZI-11) and redeposited loess material from the Zmajevac section (Z-41A–Z-42) (Figs. 9–11), probably because multiple exposure to pedogenesis.

$(Na_2O+K_2O)/Al_2O_3$ is a coefficient that represents the degree of feldspar weathering. Feldspars are dominant source material for clay minerals during pedogenesis so that the ratio represents resistance of feldspars comparing to resistant Al-oxides, i.e., intensity of pedogenesis. In all investigated profiles, the value is generally greater than 0.1. The highest values are in the loess horizons not affected by pedogenesis. In paleosols the coefficient decreases with the degree of pedogenesis because of mineral weathering (Figs. 9–11).

4.5.4. REE

Concentrations of REE in samples were normalized to chondrite (ch) (Taylor and McLennan, 1995) and the North American shale composite (NASC) (Gromet et al., 1984). Fig. 12 shows plots of REE and NASC normalized to chondrite, and a slight enrichment of REE in paleosols.

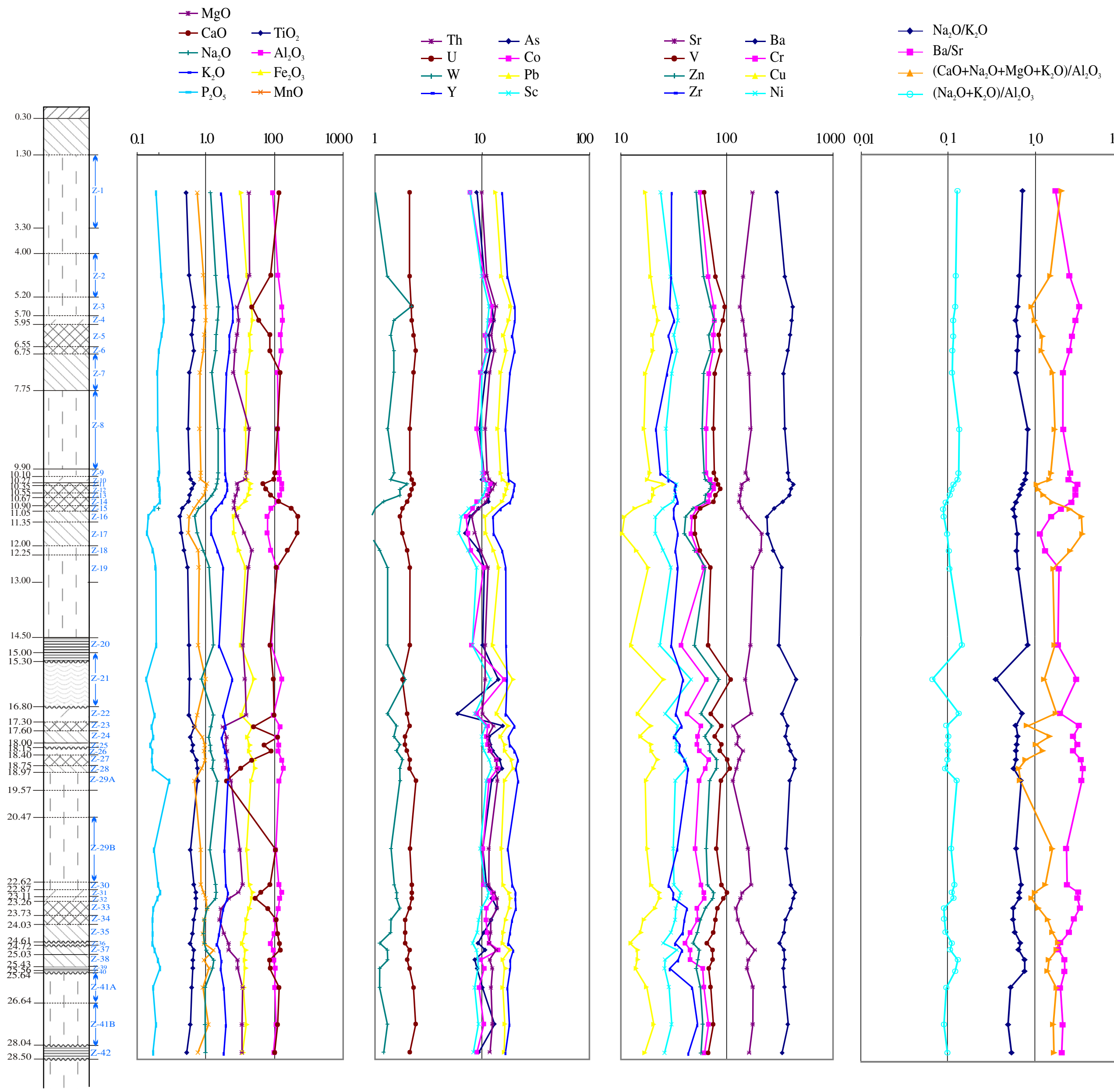

Fig. 10. Distribution of concentrations of major elements (without SiO_2 and LOI) (values in wt.%), trace elements (values in mg kg^{-1}) and weathering coefficients of the Zmajevac section; as measured by ICP-MS.

The distribution along the sections and enrichment of REE in paleosols is presented by the parameters of distribution: ΣREE, ΣLREE, ΣHREE, ΣLREE/ΣHREE, $(La/Yb)_{NASC}$ and $(La/Yb)_{ch}$ (Tables 1 and 2). The light rare earths include La, Ce, Pr, Nd and Sm, Gd, and heavy rare earths include Tb, Dy, Ho, Er, Tm, Yb and Lu.

By comparing the contents of REE among the sections, it can be noticed that in the Erdut section the lowest values are in the samples E-10–E-12A. A similar content of REE is in the Zmajevac section (Z-14–Z-18), and in Zmajevac I section ZI-10–ZI-11. In those horizons, the concentrations of REE are lower than NASC, with the exception of La in Z-11 (12).

Values, normalized to the contents of REE in chondrite, were compared to NASC and fractionation was observed. The contents of REE lighter than dysprosium is very similar to contents of those REE in NASC, but the contents of REE heavier than dysprosium are significantly lower than in NASC. Negative europium anomalies are noticed in all analyzed samples (Fig. 12). Regardless of the type of normalization, in all analyzed samples content of ΣLREE is higher than ΣHREE 10–12 times, $(La/Yb)_{NASC}$ ranges between 1.8 and 2.6 and $(La/Yb)_{ch}$ between 12 and 18 (Tables 1 and 2). Those ratios are describing the inclination of the curves (Fig. 12).

Comparing ΣREE, ΣLREE and ΣHREE, it can be noticed that these parameters have the similar distribution in the studied sections. The samples from the sections are highly enriched in all three parameters in paleosols, especially in older, pedogenetically well-developed, paleosols from the lower parts of the sections. The fact that a high content of REE is a consequence of the high degree of pedogenesis is proved by high concentrations measured in younger pedogenetically well developed paleosols from the Erdut and the Zmajevac sections. Except for those two higher concentrations, there is a general trend of increasing of the content of REE with the increase of age of the sediment. The lower values of

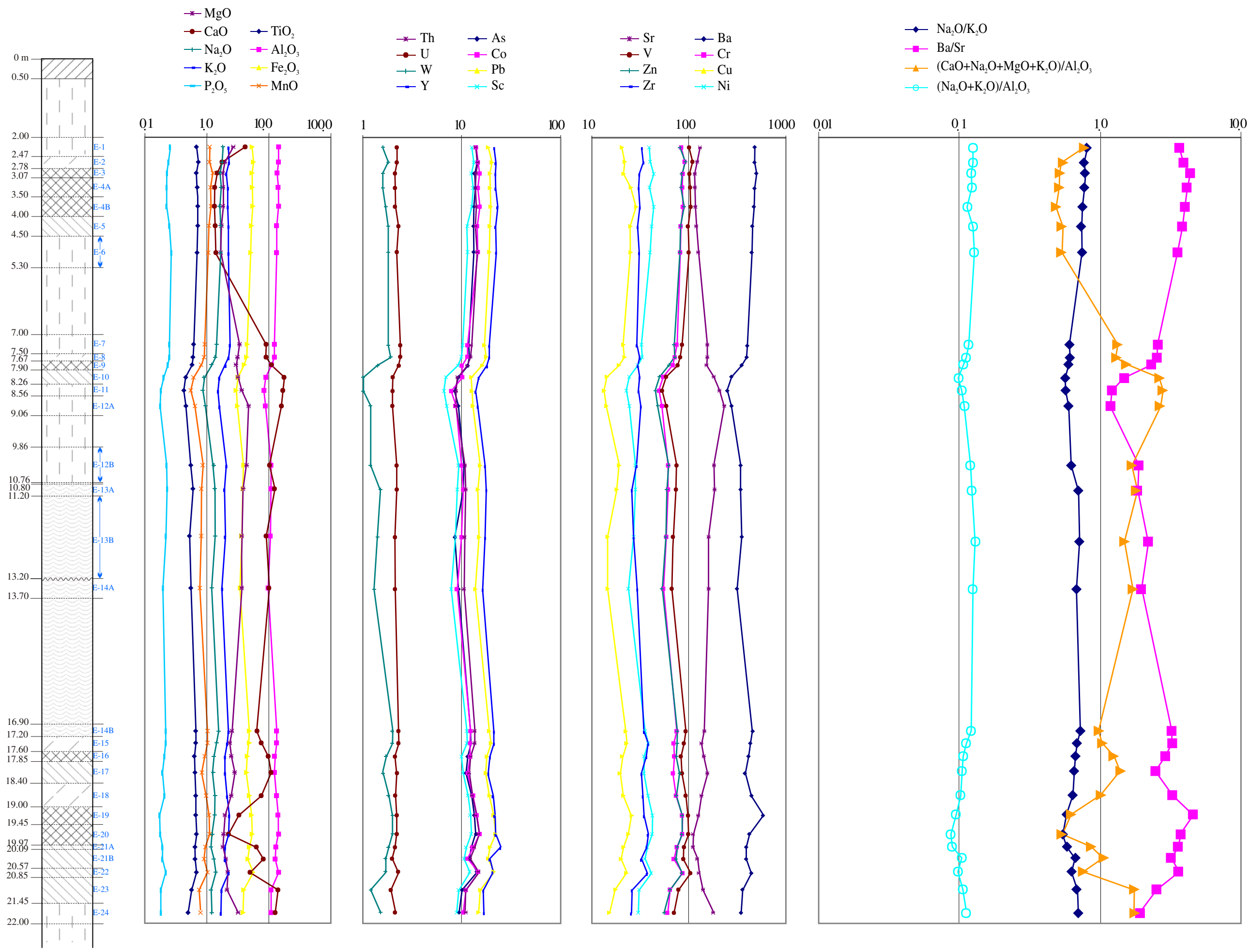

Fig. 11. Distribution of concentrations of major elements (without SiO_2 and LOI) (values in wt.%), trace elements (values in mg kg^{-1}) and weathering coefficients of the Erdut section; as measured by ICP-MS.

ΣREE were measured in loess horizons that were not affected by pedogenesis. The exceptions are the aforementioned horizons from the Erdut (E-10–E-12A) and the Zmajevac (Z-15–Z-18) sections.

4.6. Geochemical differences between loess and paleosol

Differences in correlations of achieved values between loess as parent material and paleosols (weak and well developed horizons) (see Sections 4.2–4.5) are starting point for geochemical characterization of loess and paleosols. For statistical analysis, it is necessary to define and to form homogeneous groups of samples (populations).

Since the Šarengrad section, described in Galović et al. (2011), was studied during the same field trip and by the same analytical procedures (see Section 3), this statistical analysis is supplemented by Š-1 to Š-26-horizons (n = 27). Soil sediment horizons were analyzed as well, because their transportation took place during the warm period (by water flow) and, after redeposition, they were exposed to a single or multiple pedogenesis (see Section 2). This is why they acquired geochemical characteristics of paleosols. Samples deposited in aquatic areas were excluded from statistical processing (Z-20, Z-21, Z-22, Z-39, Z-40, Z-42, E-13A, E-13B, Š-19, Š-20 and Š-21) due to significantly different geochemical environment during sedimentation. After this selection, 99 horizons were analyzed.

Those three populations (sub-groups) were statistically tested (F-test and t-test) in order to explore similarities between them. The results of t-test showed that the leaching coefficient Ba/Sr satisfies the conditions of equality of variance and mean in well-developed horizons of paleosols and weak-developed horizons of paleosols. It could not be excluded that they belong to the same population.

Based on obtained results, two sub-groups of samples were selected: loess horizons (n = 31) and paleosol horizons (n = 68) (Appendices A and B).

4.7. Discussion

Loess is (in essence) a deposit of wind-blown dust, almost totally formed by the accumulation of dust. But beside an aeolian mechanism, there is a pedological in-situ mechanism characterised by post-deposition activity (Smalley et al., 2011). Furthermore, Smalley et al. (2014) explain how this vast amount of loess material was produced. Rivers play a major role in transportation of the loess material from the source area to "storage regions" (alluvial and/or floodplain sediments). These sediments are, sometimes repeatedly, exposed to aeolian deflation, abrasion, deposition and reworking, resulting in forming loess material that has such a restricted grain-size range (Smalley et al., 2011, 2014, and references therein).

A detailed stratigraphy, supported by detailed geochronological, paleomagnetic and other data of the Danube loess from the nearby area in Vojvodina (Serbia) was presented by Marković et al. (2012,

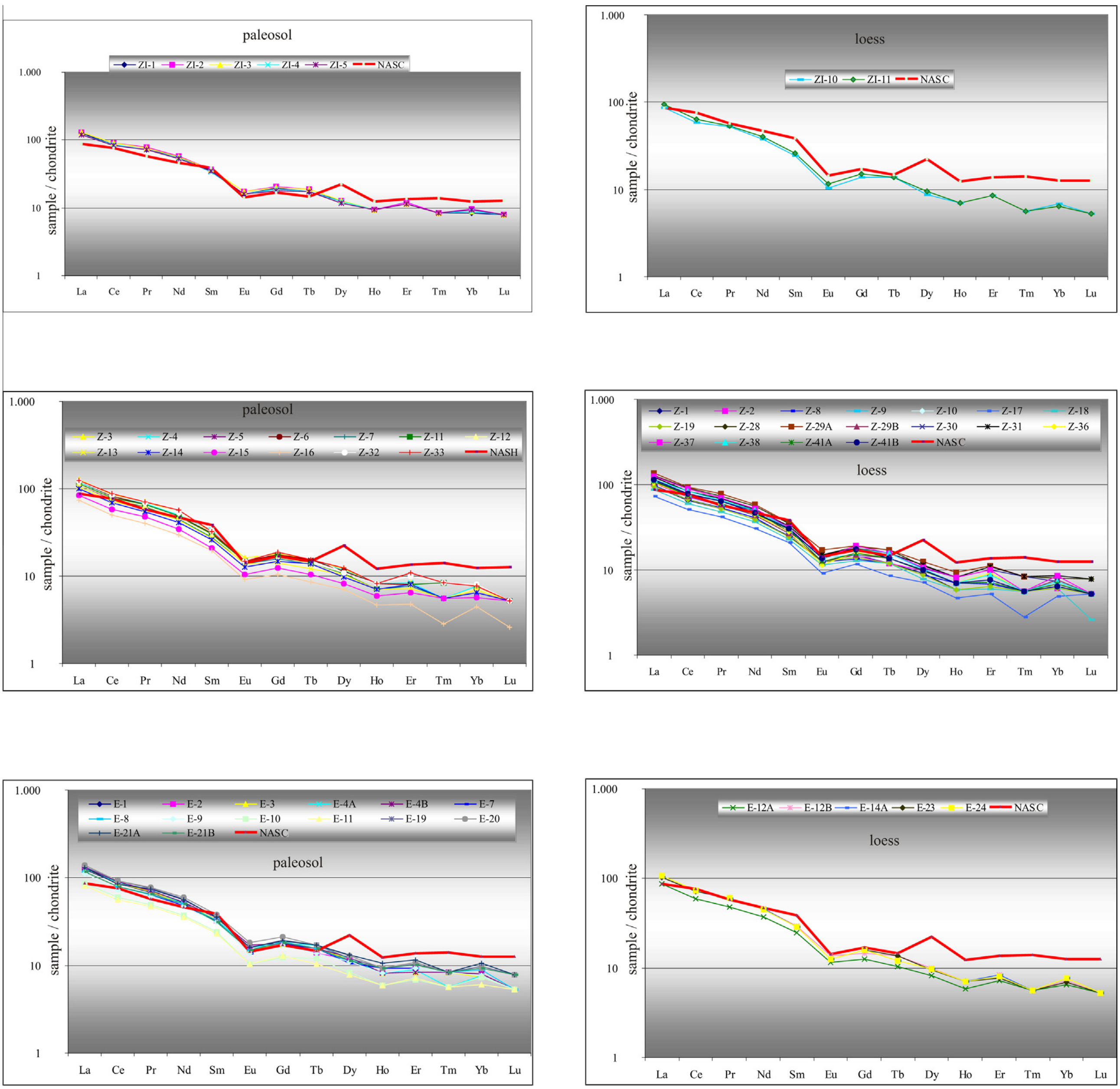

Fig. 12. Chondrite-normalized chemical analyses of REE in the samples (measured by ICP-MS) and NASC.

and references therein) and Fitzsimmons et al. (2012). Such high-resolution multi-proxy approach supported with a good geochronology is, besides for paleoclimatic reconstructions, useful for correlation and comparison of similar deposits in the area. Middle and lower Danube loess preserves continuous record of environmental change, thus variations in vegetation and malacofauna respond to climatic change (Fitzsimmons et al., 2012).

4.7.1. Geochemical distribution of major and trace elements

The geochemical compositions of loess sediments are mainly controlled by three factors: geochemistry of dust originated from different sources, grain-size sorting during transportation and post-depositional weathering (Liang et al., 2013). Based on variations of major and trace elements in different grain size fractions, it is found that Al, Fe, Mg, K, Mn, Zn, Rb, Cr, V are mainly enriched in fine size fractions, and Ti, Ba, Zr, P, Ca and Sr show irregular variations among different size fractions.

The distributions of Cu, Cr, W, Y, Pb, Bi, V and Ba in the sections under the study are strongly related to the intensity of pedogenetic processes (Figs. 3–5 and 9–11). Accumulation of those elements is supported by illuviation processes including formation of new clay minerals, translocation of elements and minerals and variations of redox conditions. High correlation coefficients between elements bonded to clay minerals and clayey grain-size fraction (Galović et al., 2009) is a result of adsorption of heavy metals on clay minerals (Adriano, 1986; Constantini et al., 2002; Hardy and Cornu, 2006). Liu et al. (2004) pointed out that chemical fractionation could also be caused by granulometric fractionation during aeolian transport. Later, Feng et al. (2011) discussed variation of geochemical composition of aeolian deposits with changes in their mineral composition as a consequence of different grain-size. They concluded that the finer sized grains such as clay minerals and accessory minerals have a relatively higher trace element concentration than the components of coarser sized grains, mainly owing to the decreasing proportion of quartz, which has a lower trace element

Table 1
Parameters of distribution of REE of the Zmajevac I and Erdut sections; as measured by ICP-MS.

Sample	Depth (cm)	ΣREE	ΣLREE	ΣHREE	ΣLREE/ΣHREE	$(La/Yb)_{NASC}$	$(La/Yb)_{ch}$
ZI-1	30–125	205.9	186.4	18.1	10.30	2.12	14.8
ZI-2	125–165	214.7	194.2	19.0	10.22	1.90	13.2
ZI-3	165–185	211.6	191.6	18.5	10.36	2.07	14.4
ZI-4	185–245	202.0	182.8	17.8	10.27	1.94	13.5
ZI-5	245–281	198.8	180.0	17.4	10.34	1.85	12.9
ZI-6	281–305	220.5	200.3	18.7	10.71	2.06	14.4
ZI-7	305–315	196.2	179.4	15.6	11.50	2.08	14.5
ZI-9	330–370	207.0	188.8	16.9	11.17	2.12	14.8
ZI-10	370–435	141.3	127.3	13.1	9.72	1.82	12.7
ZI-11	435–555	153.2	138.5	13.7	10.11	2.12	14.8
E-1	200–247	199.5	182.2	15.9	11.46	2.35	16.4
E-2	247–278	203.1	185.6	16.2	11.46	2.28	15.9
E-3	278–307	200.8	183.7	15.8	11.62	2.53	17.6
E-4A	307–350	203.6	186.1	16.1	11.56	2.40	16.7
E-4B	350–400	206.7	188.8	16.4	11.51	2.33	16.2
E-5	400–450	210.2	190.8	17.9	10.66	2.02	14.1
E-6	450–530	231.2	210.9	18.7	11.28	2.27	15.9
E-7	700–750	185.8	168.4	16.2	10.39	1.81	12.6
E-8	750–767	188.2	170.4	16.5	10.33	1.89	13.2
E-9	767–790	176.8	160.0	15.6	10.26	2.09	14.6
E-10	790–826	141.1	128.1	12.1	10.58	1.72	12.0
E-11	826–856	133.7	121.1	11.7	10.35	1.94	13.5
E-12A	856–906	140.4	127.6	11.8	10.81	1.94	13.5
E-12B	986–1076	171.6	156.4	14.0	11.17	2.10	14.6
E-13A	1080–1120	177.3	161.2	14.9	10.82	1.94	13.5
E-13B	1120–1320	164.0	149.1	13.7	10.88	2.11	14.7
E-14A	1320–1370	169.2	153.9	14.2	10.84	1.94	13.5
E-14B	1690–1720	203.8	185.1	17.4	10.64	1.86	13.0
E-15	1720–1760	202.1	183.3	17.4	10.54	1.86	13.0
E-16	1760–1785	183.6	166.9	15.5	10.77	1.94	13.5
E-17	1785–1840	176.6	160.3	15.1	10.62	1.85	12.9
E-18	1840–1900	197.5	179.4	16.7	10.74	1.82	12.7
E-19	1900–1945	215.7	196.3	18.0	10.90	1.98	13.8
E-20	1945–1997	222.8	202.4	18.8	10.76	2.15	15.0
E-21A	1997–2009	207.4	187.2	18.8	9.96	1.79	12.5
E-21B	2009–2057	189.3	171.0	17.0	10.06	1.81	12.6
E-22	2057–2085	226.3	206.3	18.5	11.15	1.98	13.8
E-23	2085–2145	168.8	153.9	13.8	11.15	2.17	15.1
E-24	2145–2200	170.9	155.7	14.1	11.05	1.99	13.9

concentration. Therefore, the grain-size effect should be considered cautiously when comparing aeolian deposits with different grain-sizes.

Statistically normal distribution of those elements implies a unique mechanism of transport. Poor and very poor sorting indicates that the material consists of a wide range of grain-sizes implying an aeolian short-distance transport. Exceptions are Ca, Sr (isomorphic exchanging of Ca by Sr in carbonates) and Mg (related to dolomite as a part of carbonates and, furthermore, having an important role in chemical composition of clay minerals). They were washed down from the upper paleosol horizons and accumulated in BC-horizons of related paleosols. Thus, these elements often show low concentrations in upper paleosol horizons. Actually, their higher concentrations are artificially decreased by sieving the fraction <2 mm, because carbonate concretions were excluded to a greater percentage. However, by analyzing the bulk sample (<2 mm), we could not avoid dilution of heavy metal contents by approximately 15–25% of $CaCO_3$ in BC-horizons (Figs. 9–11) and increase of heavy metal concentrations in the almost carbonate-free upper part of the Erdut section (Figs. 8 and 11). This explains the local maximum concentration of heavy metals in cumulic and B-horizons as well as decreasing values with depth towards BC-horizons of related paleosols resulting in significant negative correlation between Ca, Sr and Mg on the one side and all other analyzed major and trace elements on the other side. Therefore, the most important mechanisms of distribution of major and trace elements in studied loess sections are argillization and carbonate translocation.

Assuming that pedogenetically well-developed paleosols are enriched with Fe, K, Mn, Ti and trace elements with lower mobility, a conclusion is that the older paleosols are better developed. Constantini et al. (2002) analyzed the chemical composition of modern soils and Pleistocene paleosols. They identified a general enrichment trend of Fe, Cr and Pb in paleosols with age, while Ca in paleosols decreases with age. Buggle et al. (2011) emphasize that distribution of some elements might be controlled by redox conditions, also after burial of the paleosol. For this reason, they suggest that the use of the elements Fe and Mn in weathering studies is not recommended.

Comparing the chemical composition from Appendices A and B with results determined by similar analytical chemical methods for loess/paleosol sequences from other countries (Norway, Argentina, Croatia, USA, China, Serbia, Romania, Ukraine, Germany, Hungary, New Zeeland), a similar range of concentrations is found (Gallet et al., 1998; Durn et al., 1999; Driese et al., 2000; Ding et al., 2001; Jahn et al., 2001; Munroe et al., 2007; Buggle et al., 2008, 2011; Újvári et al., 2008, 2014; Feng et al., 2011).

4.7.2. Geochemical distribution of REE

Feng et al. (2011) studied variations in trace element (including REE) concentrations with grain sizes in loess and their implications for tracing the provenance of aeolian deposits. They proved that the finer sized grains, such as clay minerals and accessory minerals, have a relatively higher trace element concentration than the components of coarser sized grains, mainly

Table 2
Parameters of distribution of REE of the Zmajevac section; as measured by ICP-MS.

Sample	Depth (cm)	ΣREE	ΣLREE	ΣHREE	ΣLREE/ΣHREE	$(La/Yb)_{NASC}$	$(La/Yb)_{ch}$
Z-1	130–330	152.8	138.9	12.8	10.85	2.26	15.8
Z-2	400–520	166.1	151.7	13.2	11.49	2.45	17.1
Z-3	520–570	200.7	183.2	16.1	11.38	2.40	16.7
Z-4	570–595	191.5	174.5	15.7	11.11	2.24	15.6
Z-5	595–655	178.4	162.4	14.7	11.05	2.48	17.3
Z-6	655–675	190.7	173.9	15.5	11.22	2.42	16.9
Z-7	675–775	176.6	161.2	14.2	11.35	2.34	16.3
Z-8	775–990	156.0	142.6	12.3	11.59	2.33	16.2
Z-9	990–1010	168.3	153.7	13.4	11.47	2.52	17.6
Z-10	1010–1027	171.5	156.7	13.6	11.52	2.42	16.9
Z-11	1027–1035	185.0	168.6	15.1	11.17	2.14	14.9
Z-12	1035–1055	179.3	163.5	14.6	11.20	2.21	15.4
Z-13	1055–1067	167.6	152.9	13.5	11.32	2.17	15.1
Z-14	1067–1090	160.0	145.3	13.6	10.68	2.24	15.6
Z-15	1090–1105	134.1	121.8	11.4	10.69	2.15	15.0
Z-16	1105–1135	115.6	105.5	9.3	11.35	2.38	16.6
Z-17	1135–1200	119.6	108.8	10	10.88	2.18	15.2
Z-18	1200–1225	139.9	127.5	11.4	11.19	2.07	14.4
Z-19	1225–1300	152.9	139.5	12.3	11.34	2.26	15.8
Z-20	1450–1500	169.0	153.6	14.3	10.74	2.17	15.1
Z-21	1500–1680	145.5	130.8	13.6	9.61	1.72	12.0
Z-22	1680–1730	157.2	142.8	13.3	10.74	1.99	13.9
Z-23	1730–1760	197.0	179.1	16.6	10.79	2.18	15.2
Z-24	1760–1800	174.7	158.8	14.7	10.80	2.22	15.5
Z-25	1800–1815	177.9	161.7	15	10.78	2.15	15.0
Z-26	1815–1840	183.0	165.8	16	10.36	2.14	14.9
Z-27	1840–1875	209.3	189.8	18.1	10.49	1.90	13.2
Z-28	1875–1897	210.3	192.0	17	11.29	2.28	15.9
Z-29A	1897–1957	220.0	200.7	17.8	11.28	2.31	16.1
Z-29B	2047–2262	169.9	154.5	14.3	10.80	1.99	13.9
Z-30	2262–2287	181.3	164.3	15.7	10.47	2.21	15.4
Z-31	2287–2311	196.4	178.2	16.9	10.54	2.08	14.5
Z-32	2311–2326	199.2	181.0	16.9	10.71	2.18	15.2
Z-33	2326–2373	205.7	187.2	17.2	10.88	2.35	16.4
Z-34	2373–2403	185.5	168.5	15.8	10.66	2.14	14.9
Z-35	2403–2461	178.4	162.3	14.9	10.89	2.04	14.2
Z-36	2461–2472	172.4	156.9	14.5	10.82	2.17	15.1
Z-37	2472–2503	203.9	186.2	16.5	11.28	2.12	14.8
Z-38	2503–2543	190.0	173.6	15.2	11.42	2.26	15.8
Z-40	2556–2564	193.6	177.5	14.8	11.99	2.66	18.6
Z-41A	2564–2664	173.5	158.6	13.8	11.49	2.28	15.9
Z-41B	2664–2804	181.2	165.6	14.4	11.50	2.54	17.7
Z-42	2804–2850	170.4	155.9	13.4	11.64	2.36	16.5

Table 3
Sub-groups of samples selected according to the degree of soil development distinguished based on TOC values.

Well developed horizons of paleosols			Weak developed horizons of paleosols		Loess	
Z-I 1	Z-32	Š-3	Z-I 6	E-18	Z-I 10	Z-37
Z-I 2	Z-33	Š-4	Z-I 7	E-22	Z-I 11	Z-38
Z-I 3	E-1	Š-8	Z-I 9	Š-2	Z-1	Z-41A
Z-I 4	E-2	Š-9	Z-23	Š-5	Z-2	Z-41B
Z-I 5	E-3	Š-14	Z-24	Š-6	Z-8	E-12A
Z-3	E-4A	Š-15	Z-25	Š-7	Z-9	E-12B
Z-4	E-4B	Š-16	Z-26	Š-10	Z-10	E-14A
Z-5	E-7	Š-17A	Z-27	Š-13	Z-17	E-23
Z-6	E-8	Š-17B	Z-34	Š-24	Z-18	E-24
Z-7	E-9		Z-35	Š-25	Z-19	Š-1
Z-11	E-10		E-5	Š-26	Z-28	Š-11
Z-12	E-11		E-6		Z-29A	Š-12
Z-13	E-19		E-14B		Z-29B	Š-18
Z-14	E-20		E-15		Z-30	Š-22
Z-15	E-21A		E-16		Z-31	Š-23
Z-16	E-21B		E-17		Z-36	

owing to the decreasing proportion of quartz, which has a lower trace element concentration. Therefore, the variations in REE and other trace element concentrations with grain sizes can likely be attributed to the proportional change of various minerals from weathering processes and late mineral sorting.

REEs are widely used in the provenance characterization of aeolian sediments around the world (Taylor and McLennan, 1995; Yang et al., 2007; Muhs et al., 2010) with similar distribution pattern. The REE distribution patterns achieved in this study is analogous to distribution and composition of loess sediments in the Ili

Basin, Central Asia (Song et al., 2014). The authors indicate that loess is of typical upper crustal compositions, with enrichment in LREE, negative Eu anomalies and depletion of HREE.

LREE/HREE and La_N/Yb_N (chondrite-normalized data) reflect the fractionation of HREE and LREE. Although REEs are usually relatively immobile elements, there is evidence showing that HREE are mobilized to a greater extent than are the LREE. The chondrite-normalized REE distribution patterns are rather uniform, characterized by steep LREE and relatively flat HREE patterns and by persistent negative Eu anomalies (Fig. 12) (Hao et al., 2010; Jahn et al., 2001; Muhs and Budahn, 2009; Muhs et al., 2007, 2010; Sun et al., 2007).

4.7.3. Geochemical distribution of TOC

Whether horizon have been affected by pedogenesis was determined on the basis of TOC content and S_o/S_k (in Š-24–Š-26 with low TOC, but the most of other measured and counted parameters indicate intensive pedogenesis (Galović et al., 2011)). In paleosol horizons the population has TOC > 0.15%. TOC > 0.2% was identified in pedogenetically well-developed horizons (mostly B-horizons). Horizons with TOC < 0.15% belong to the loess population, and horizons with TOC value between 0.15% and 0.2% belong to the sub-group of weak-developed paleosol horizons-mostly cumulic and BC-horizons) (Table 3).

TOC contents in loess/paleosol section Crvenka, Serbia (Zech et al., 2013) are higher than values in this study, but have the same loess–paleosol ratio and they concluded that TOC can be used to identify paleosols and to characterize the *intensity* of pedogenesis. Antoine et al. (2009) based on research in loess–paleosol section Surduk, Serbia, notice that variations in TOC percentage reinforcing the opposition between periods of pure loess deposition (low TOC percentage) and periods of pedogenesis (high TOC percentage). Furthermore, comparison between the clay, TOC, MS and coarse particle variations allows reinforcing the differentiation between the various soil and soil complexes within the sequence. The combination of clay, TOC and MS variations is thus very useful to define an accurate sedimentological signature of the various types of soils (Chernozem, cambic horizons) and can be used as a good proxy for local temperature and moisture reconstructions (Antoine et al., 2009). Further investigation of vegetation on the same section by Hatté et al. (2013) suggests a strong meridional Mediterranean circulation schema over Europe with a focus on Balkan areas. This climatic configuration would have led to short and very dry summer conditions unfavourable to C3 plant development and, therefore, would have allowed the development of C4 plants (Hatté et al., 2013).

4.7.4. Weathering coefficients

During pedogenesis of non-carbonated parent material, plagioclase minerals are the least resistant to weathering (Yingjun and Congqiang, 1999). Ca is more often in calcite than in plagioclase structures. The applied weathering indices (Kahmann and Driese, 2008; Buggle et al., 2008, 2011; Boguckyj et al., 2009; Bokhorst et al., 2009; Galović et al., 2011; Újvári et al., 2014) to indicate the degree of pedogenesis (Figs. 9–11). Mirror curves of Ba/Sr and $(CaO+Na_2O+MgO+K_2O)/Al_2O_3$ demonstrate that the loss of bases correlates with sediment leaching and the duration of pedogenesis. More specifically, as an indicator for rainfall and precipitation amount that favour leaching of these elements from primary minerals (Bokhorst et al., 2009). Based on those two coefficients and S_o/S_k ratios, some paleosols (E-23–E18, could be recognized as pedocomplexes, containing two B-horizons. Furthermore, for each paleosol, the degree of pedogenetic development can be realized.

The other two coefficients $[(Na_2O+K_2O)/Al_2O_3$ and $(Na_2O/K_2O)]$ indicate that amounts of both plagioclases and feldspars, decrease with depth within each paleosol. This demonstrates that all paleosol horizons are weathered, even though the leaching coefficient and base loss index emphasize weathering of the upper part of the paleosol horizons only. Rubinić et al. (2014, XXXX) analyzed the precipitation gradient in modern pseudogley developed on loess in the Pannonian region applying different weathering indices. Within all analyzed profiles, CIA values are generally increased with depth. In a record of chemical weathering in the Paks loess–paleosol sequence it is noted that all weathering ratios and indices, except for TiO_2-normalized one, exhibit a slight decrease from the OLS to the YLS (Újvári et al., 2014).

Compared to weathering coefficients from the Istrian terra rossa (Durn et al., 1999), these paleosols have two to three times higher $(CaO+Na_2O+MgO+K_2O)/Al_2O_3$ ratios and distinctively lower Ba/Sr ratio, because of higher weathering intensity of red clay pedogenesis (Bt-horizon).

Appendix A

Elementary statistics for loess-population (values expressed in mg kg^{-1} except: Ag – values expressed in mg t^{-1} and * – values expressed in %).

Loess n = 31	$\bar{X}$	Median	SD	Min	Max
Ag	55.00	54.00	13.43	32.00	85.00
Al*	5.69	5.74	0.85	4.05	7.08
As	10.75	10.20	1.97	7.00	15.40
Ba	354.45	353.00	50.95	242	442
Bi	0.22	0.22	0.04	0.15	0.3
Ca*	7.57	7.39	2.84	1.43	15.36
Cd	0.16	0.15	0.03	0.09	0.22
Co	10.50	10.30	1.84	7.4	14.2
Cr	58.23	61.00	9.96	38	76
Cu	17.82	17.70	3.30	10.28	25.16
Fe*	2.82	2.80	0.47	1.86	3.75
K*	1.51	1.54	0.20	1.00	1.85
Mg*	2.00	2.04	0.49	1.12	2.87
Mn	650.65	657.00	107.03	424.00	990.00
Mo	0.45	0.44	0.07	0.35	0.65
Na*	0.86	0.87	0.16	0.519	1.119
Ni	30.17	29.70	5.07	21.1	41.5
P*	0.07	0.06	0.01	0.048	0.102
Pb	15.64	15.51	2.19	10.86	20.57
Sb	0.84	0.83	0.12	0.6	1.12
Sc	9.32	9.20	1.48	6.1	12.3
Sn	2.37	2.40	0.40	1.8	3.3
Sr	162.45	160.0	26.55	114	233
Th	11.44	11.40	1.43	8.5	14.6
Ti*	0.36	0.35	0.05	0.264	0.46
U	2.10	2.10	0.14	1.8	2.4
V	76.16	75.00	13.44	50	106
W	1.34	1.30	0.22	0.8	1.7
Zn	60.94	61.10	10.17	39.9	80.5
Zr	34.37	33.00	7.67	21.3	52.7
Y	17.58	17.30	1.93	12.8	21.6
La	39.29	39.00	4.97	27	50
Ce	70.95	70.14	9.48	49.48	89.8
Pr	8.31	8.30	1.11	5.7	10.6
Nd	32.58	32.30	4.56	21.8	42
Sm	6.64	6.60	0.82	4.8	8.3
Eu	1.17	1.20	0.16	0.8	1.5
Gd	4.83	4.80	0.59	3.6	5.8
Tb	0.81	0.80	0.12	0.5	1
Dy	3.80	3.80	0.47	2.7	4.8
Ho	0.62	0.60	0.09	0.4	0.8
Er	2.10	2.10	0.39	1.3	2.8
Tm	0.23	0.20	0.05	0.1	0.3
Yb	1.79	1.80	0.28	1.2	2.4
Lu	0.21	0.20	0.04	0.1	0.3
Hf	1.15	1.07	0.24	0.78	1.72
Li	33.11	32.00	5.83	23.6	47.7
Rb	82.97	84.00	12.87	54.4	114.4
Nb	7.09	6.89	1.07	5.28	9.53
Cs	4.35	4.30	0.75	2.9	6
Ga	13.76	13.65	2.26	9.04	18.29

Appendix B
Elementary statistics for paleosol-population (values expressed in mg kg^{-1} except: Ag – values expressed in mg t^{-1} and * – values expressed in %).

Paleosol n = 68	$\overline{X}$	Median	SD	Min	Max
Ag	58.28	58.00	12.62	25	86
Al*	6.56	6.57	0.81	4.14	7.97
As	12.55	12.30	2.39	6.5	23.7
Ba	405.76	400.00	58.65	238	576
Bi	0.27	0.27	0.04	0.15	0.36
Ca*	4.91	4.70	3.36	0.72	15.51
Cd	0.16	0.16	0.03	0.1	0.25
Co	12.45	12.00	2.10	7.1	16.5
Cr	71.07	71.00	12.15	45	93
Cu	21.47	21.09	3.92	10.73	29.97
Fe*	3.29	3.26	0.46	1.85	4.04
K*	1.66	1.69	0.22	0.99	2.13
Mg*	1.40	1.41	0.30	0.95	2.22
Mn	717.25	725.50	150.64	381	1032
Mo	0.43	0.43	0.06	0.21	0.54
Na*	0.91	0.91	0.19	0.51	1.33
Ni	35.75	35.40	5.37	21.2	52.1
P*	0.07	0.07	0.01	0.049	0.092
Pb	18.42	18.23	3.04	10.61	27.13
Sb	0.91	0.90	0.13	0.59	1.27
Sc	10.80	10.90	1.43	6.3	13.4
Sn	2.89	3.00	0.36	1.7	3.5
Sr	129.24	128.50	19.84	100	205
Th	12.95	12.90	1.76	7.9	16.9
Ti*	0.39	0.40	0.04	0.248	0.451
U	2.15	2.15	0.18	1.7	2.5
V	88.12	89.00	12.32	50	108
W	1.64	1.70	0.27	0.8	2.2
Zn	72.60	72.80	10.95	41	98.7
Zr	36.48	34.85	6.76	27.4	55.7
Y	19.82	20.05	2.19	12.6	24.5
La	43.78	44.50	5.16	27	54
Ce	79.00	80.07	9.64	47.62	96.29
Pr	9.31	9.45	1.14	5.5	11.2
Nd	36.42	36.60	4.59	20.9	43.8
Sm	7.46	7.60	0.94	4.5	9.2
Eu	1.31	1.30	0.17	0.8	1.6
Gd	5.36	5.40	0.64	3.2	6.5
Tb	0.92	0.90	0.13	0.5	1.1
Dy	4.35	4.40	0.51	2.7	5.2
Ho	0.72	0.70	0.09	0.4	0.9
Er	2.37	2.40	0.35	1.2	3
Tm	0.27	0.30	0.05	0.1	0.3
Yb	2.08	2.10	0.31	1.1	2.6
Lu	0.25	0.20	0.05	0.1	0.3
Hf	1.25	1.21	0.23	0.92	1.85
Li	39.27	39.15	5.60	23.1	50.4
Rb	99.58	98.20	14.98	55.7	133.8
Nb	8.07	8.14	0.94	5.09	9.71
Cs	5.22	5.15	0.87	2.9	7.6
Ga	16.10	16.36	2.16	8.91	20.49

Gallet et al. (1998) noted that most or all worldwide loesses are derived from protoliths that have undergone at least one cycle (and probably *many* cycles) of weathering, pedogenesis, or diagenesis prior to aeolian entrainment, transport, and deposition as loess. Thus, the lower Na_2O/Al_2O_3 values of the loess maybe inherited from the "preweathered" sediments or sedimentary rocks that served as the source of the loess and displayed at least some degree of Na-plagioclase depletion (Muhs and Budahn, 2006).

4.7.5. Identifying the origin of source of material

Oreščanin et al. (2005) studied recent channel sediments of the Danube River in the village of Batina (upstream boundary point of the study area in this investigation). Alluvial sediments are mainly composed of muddy, fine to medium sand. It was found that the greatest proportion of the total heavy metal load is contained in the clay and silt fraction, and therefore sediment metal transport appears to be governed primarily by sorption–desorption processes associated with fine-grained particles. A comparison of the total Pb, Cu, Zn, Cr, Mn, Fe and Ni concentrations with the average shale and soil composition suggests that the analysed metals represent mostly natural levels in the investigated sediments and are not characterized by emissions of untreated wastewater in Budapest to any extent. Geochemical content of grain-size fraction B (0.063–0.25 mm) (Orešcanin et al., 2005) is in the ranges indentified for the loess subgroup (Appendix A) for Pb, Cu, Zn and Ni. Analyzed B-fraction of recent channel sediments of the Danube Rover are enriched with Cr and have minor Mn and Fe than loess sediments studied in this investigation. This allows possibility of the other alluvial source material for aeolian sedimentation than the Danube River.

Buggle et al. (2008) geochemically characterized the loess/paleosol sections of Batajnica/Stari Slankamen (Serbia), Mircea Voda (Romania) and Stary Kaydaky (Ukraine) in order to identify origin of South-eastern and Eastern European loesses. They concluded that the Danube catchment area is the most important for the Pleistocene delivery of silt-sized alluvial sediments in the area. However, they considered also the Drava River as further important silt source, supplying glacio-fluvial sediments of the Eastern Alps with respect to element composition and weathering products (see Section 2) (Buggle et al., 2008).

Banak et al. (2013) investigated mineral composition of heavy mineral fraction in the Zmajevac. They concluded that such high portion of amphiboles could be consequence of denudation from locally exposed volcanic and metamorphic rocks of the southward neighbouring Slavonian Mts. (Balen et al., 2006). Krndija and Papuk Mts. are the closest to Baranja of all the Slavonian Mts which are composed of amphibolites. Furthermore, Pliocene sands from the northern slopes of Krndija and Papuk Mts. are of local origin and contain abundant amphiboles (Balen et al., 2006).

A record of chemical weathering of the Paks loess–paleosol sequence (Hungary) proved the appearance of amphiboles while high dolomite contents suggest that loess material was at least partly sourced from local rocks. Simultaneously, geochemical data reveal a genetic link between floodplain sediments and loess deposits (Újvári et al., 2014).

The extreme Md value in cumulic E-15 horizon (Fig. 8) is a consequence of >80% course-grained silt indicating different (most probable local) source material of aeolian deposit. However, extreme value of the single sample cannot be the proof, but could support the hypothesis of influence of local source of material.

5. Conclusions

Assuming that pedogenetically strongly developed paleosols are enriched with Al, Fe, K, Mn, Na, Ti, P, and trace elements with lower mobility (As, Co, Sc, Th, Cu, Cr, W, Y, Nb, Sn, Pb, Bi, Li, Ni, Rb, Zn, V, Ga, Ba and Sb), the older paleosols are better developed indicating that during their pedogenesis climate was more humid and warmer than in later warming periods.

Paleosol horizons could be clearly separated based on weathering coefficients of Ba/Sr and $(CaO+Na_2O+MgO+K_2O)/Al_2O_3$. Weathering was most intensive in the surface paleosol horizons, with decreasing intensity towards the BC-horizons, which have the highest carbonate content.

The clay fraction is higher in paleosol horizons, especially in older well-developed paleosol where pedogenic processes were intensive.

The presence of crotovinas filled with soil material from paleosols not present in the record indicates erosion of paleosols, thus leaving an incomplete record. Furthermore, carbonate horizons without associated well developed paleosol support this claim.

Loess horizons contain <0.1% of TOC, while paleosol horizons contain between 0.1% and 0.5% of TOC. Sub-groups of samples selected according to the degree of soil development can be distinguished according to the TOC values, results of *F*- and *t*-tests show that weathering coefficient of Ba/Sr fits the criteria of equality of variances and means in less developed paleosols and paleosols. Accordingly, possibility cannot be rejected that two sub-groups of samples belong to the same population.

Loess material is at least partly derived from local rocks, alluvial sediments and loess deposits.

Acknowledgments

The work was supported by Project Nr. 181-1811096-1181 of the Croatian Ministry of science, education and sports. The author hereby expresses her thankfulness to Zoran Peh, Manfred Frechen, Goran Durn and Josip Halamić for help and advice and to Zoran Peh for language improvements. I am grateful to Jan-Berend Stuut and to anonymous reviewer for their constructive and highly valuable reviews that greatly helped to strongly improve my manuscript.

Appendix

See Appendixes A and B.

References

Adriano, D.C., 1986. Trace Elements in the Terrestrial Environment. Springer Verlag, Berlin, Heidelberg.
Antoine, P., Rousseau, D.D., Fuchs, M., Hatté, C., Gauthier, C., Marković, S.B., Jovanović, M., Gaudenyi, T., Moine, O., Rossignol, J., 2009. High-resolution record of the last climatic cycle in the southern Carpathian Basin (Surduk, Vojvodina, Serbia). Quat. Int. 198, 19–36.
Bačani, A., Šparica, M., Velić, J., 1999. Quaternary deposits as the hydrogeological system of Eastern Slavonia. Geol. Croat. 52 (2), 141–152.
Balen, D., Horvath, P., Tomljenović, B., Finger, F., Humer, B., Pamić, J., Arkai, P., 2006. A record of pre-Variscan Barrovian regional metamorphism in the eastern part of the Slavonian Mountains (NE Croatia). Mineral. Petrol. 87, 143–162.
Banak, A., Mandić, O., Kovačić, M., Pavelić, D., 2012. Late Pleistocene climate history of the Baranja loess plateau – evidence from the Zmajevac loess–paleosol section (northeastern Croatia). Geol. Croat. 65 (3), 411–422.
Banak, A., Pavelić, D., Kovačić, M., Mandić, O., 2013. Sedimentary characteristics and source of loess in Baranja (Eastern Croatia). Aeolian Res. 11, 129–139.
Boguckyj, A.B., Łanczont, M., Łącka, B., Madeyska, T., Nawrocki, J., 2009. Quaternary sediment sequence at Skala Podil'ska, Dniester River basin (Ukraine): preliminary results of multi-proxy analyses. Quat. Int. 198, 173–194.
Bokhorst, M.P., Beets, C.J., Marković, S.B., Gerasimenko, N.P., Matviishina, Z.N., Frechen, M., 2009. Pedo-chemical climate proxies in Late Pleistocene Serbian–Ukranian loess sequences. Quat. Int. 198, 113–123.
Bronger, A., 1976. Zur quartären Klima- und Landschaftsentwicklung des Karpatenbeckens auf (palaeo)-Pedologischer und Bodengeographischer Grundlage. Kieler Geographische Schriften 45.
Bronger, A., 2003. Correlation of loess–paleosol sequences in East and Central Asia with SE Central Europe: towards a continental Quaternary pedostratigraphy and paleoclimatic history. Quat. Int. 106–107, 11–31.
Buggle, B., Glaser, B., Zöller, L., Hambach, U., Marković, S., Glaser, I., Gerasimenko, N., 2008. Geochemical characterization and origin of Southeastern and Eastern European loesses (Serbia, Romania, Ukraine). Quat. Sci. Rev. 27 (9–10), 1058–1075.
Buggle, B., Glaser, B., Hambach, U., Gerasimenko, N., Marković, S., 2011. An evaluation of geochemical weathering indices in loess–paleosol studies. Quat. Int. 240, 12–21.
Constantini, E.A.C., Angelone, M., Napoli, R., 2002. Soil geochemistry and pedological processes. The case study of the Quaternary soils of the Montagnola Senese (Central Italy). Il Quarernario 15, 53–68.
CGS-Department for Geology, 2009. Geological Map of Republic of Croatia, M 1:300.000. Croatian Geological Survey, Department for Geology, Zagreb.
Darnley, A.G., Björklund, A., Bølviken, B., Gustavsson, N., Koval, P.V., Plant, J.A., Steenfelt, A., Tauchid, M., Xie, X., Garrett, R.G., Hall, G.E.M., 1995. A Global Geochemical Database for Environmental and Resource Management: Recommendations for International Geochemical Mapping. Final Report of IGCP Project 259, 2nd revised ed. UNESCO, Paris.
Ding, Z.L., Sun, J.M., Yang, S.L., Liu, T.S., 2001. Geochemistry of the Pliocene red clay formation in the Chinese Loess Plateau and implications for its origin, source provenance and paleoclimate change. Geochim. Cosmochim. Acta 65 (6), 901–913.
Driese, S.G., Mora, C.I., Stiles, C.A., Joeckel, R.M., Nordt, L.C., 2000. Mass-balance reconstruction of a modern Vertisol; implications for interpreting the geochemistry and burial alteration of paleo-Vertisols. Geoderma 95 (3–4), 179–204.
Durn, G., Ottner, F., Slovenec, D., 1999. Mineralogical and geochemical indicators of the polygenetic nature of terra rossa in Istria. Geoderma 91 (1–2), 125–150.
Feng, J.L., Hu, Z.G., Ju, J.T., Zhu, L.P., 2011. Variations in trace element (including rare earth element) concentrations with grain sizes in loess and their implications for tracing the provenance of eolian deposits. Quat. Int. 240, 116–126.
Fitzsimmons, K.E., Marković, S.B., Hambach, U., 2012. Pleistocene environmental dynamics recorded in the loess of the middle and lower Danube basin. Quat. Sci. Rev. 41, 104–118.
Folk, R.L., 1974. The Petrology of Sedimentary Rocks. Hemphill Publishing Co., Austin, Texas.
Frechen, M., Pécsi, M., 2004. Abony brickyard: IRSL and TL analysis of "Infusion Loess". LoessInForm 4, 63–70, Budapest.
Gallet, S., Jahn, B., Van Vliet Lanoë, B., Dia, A., Rossello, E., 1998. Loess geochemistry and its implications for particle origin and composition of the upper continental crust. Earth Planet. Sci. Lett. 156, 157–172.
Galović, I., Mutić, R., 1984. Gornjopleistocenski sedimenti istočne Slavonije (Hrvatska). Rad JAZU 411, 299–356, Zagreb, (in Croatian).
Galović, L., Frechen, M., Halamić, J., Durn, G., Romić, M., 2009. Loess chronostratigraphy in Eastern Croatia – a luminescence dating approach. Quat. Int. 198, 85–97.
Galović, L., Frechen, M., Peh, Z., Durn, G., Halamić, J., 2011. Loess/paleosol section in Šarengrad, Croatia – a qualitative discussion on the correlation of the geochemical and magnetic susceptibility data. Quat. Int. 240 (1–2), 22–34.
Galović, L., Peh, Z., 2014. Eeolian contribution to geochemical and mineralogical characteristics of some soil types in Medvednica Mountain, Croatia. Catena 117, 145–156.
Gorjanović-Kramberger, D., 1912. Iz prapornih predjela Slavonije. Vijesti geol. povjerensztva 2, 28–30, Zagreb, (in Croatian).
Gorjanović-Kramberger, D., 1914. Iz prapornih predjela Slavonije. Vijesti Geol. povjerenszva 3–4, 21–26, Zagreb, (in Croatian).
Gromet, L.P., Haskin, L.A., Korotev, R.L., Dymek, R.F., 1984. The "North American shale composite": its compilation, major and trace element characteristics. Geochim. Cosmochim. Acta 48, 2469–2482.
Halamić, J., Galović, L., Šparica, M., 2003. Heavy Metal (As, Cd, Cu, Hg, Pb and Zn) distribution in topsoil developed on alluvial sediments of the Drava and Sava Rivers in NW Croatia. Geol. Croat. 56 (2), 215–232.
Halamić, J., Peh, Z., Miko, S., Galović, L., Šorša, A., 2012. Geochemical Atlas of Croatia: environmental implications and geodynamical thread. J. Geochem. Explor. 115, 36–46.
Hao, Q., Guo, Z., Qiao, Y., Xu, B., Oldfield, F., 2010. Geochemical evidence for the provenance of middle Pleistocene loess deposits in southern China. Quat. Sci. Rev. 29 (23–24), 3317–3326.
Hardy, M., Cornu, S., 2006. Location of natural trace elements in silty soils using particle-size fractionation. Geoderma 133, 295–308.
Hatté, C., Gauthier, C., Rousseau, D.-D., Antoine, P., Fuchs, M., Lagroix, F., Markovich, S.B., Moine, O., Sima, A., 2013. Excursions to C4 vegetation recorded in the Upper Pleistocene loess of Surduk (Northern Serbia): an organic isotope geochemistry study. Clim. Past Discuss. 9, 187–215.
HRN ISO 10693, 2004. Soil quality – determination of carbonate content – volumetric method.
HRN ISO 11277, 2004. Soil quality – determination of particle size distribution in mineral soil material – method by sieving and sedimentation.
Hupuczi, J., Molnár, D., Galović, L., Sümegi, P., 2010. Preliminary malacological investigation of the loess profile at Šarengrad, Croatia. Central Eur. J. Geosci. 2 (1), 57–63.
Jahn, B., Gallet, S., Han, J., 2001. Geochemistry of Xining, Xifeng and Jixan sections, Loess Plateau of China: eolian dust provenance and paleosol evolution during the last 140 ka. Chem. Geol. 178, 71–94.
Kahmann, J.A., Driese, S.G., 2008. Paleopedology and geochemistry of Late Mississippian (Chesterian) Pennington Formation paleosols at Pound Gap, Kentucky, USA: implications for high-frequency climate variations. Palaeogeogr. Palaeoclimatol. Palaeoecol. 259, 357–381.
Liang, L., Sun, Y., Beets, C.J., Prins, M.A., Wu, F., Vandenberghe, J., 2013. Impacts of grain size sorting and chemical weathering on the geochemistry of Jingyuan loess in the northwestern Chinese Loess Plateau. J. Asian Earth Sci. 69, 177–184.
Liu, L.W., Chen, J., Chen, Y., Ji, J.F., 2004. Wind sorting and chemical weathering effects on element concentrations in the Chinese loess and its implications for paleoclimate change. Goldschmidt 2004, A438, Copenhagen.
Marković, S.B., Hambach, U., Catto, N., Jovanović, M., Buggle, B., Machalett, B., Zöller, L., Glaser, B., Frechen, M., 2009. Middle and late Pleistocene loess sequences at Batajnica, Vojvodina, Serbia. Quat. Int. 198, 255–266.
Marković, S.B., Hambach, U., Stevens, T., Kukla, G.J., Heller, F., McCoy, W.D., Oches, E.A., Buggle, B., Zöller, L., 2011. The last million years recorded at the Stari Slankamen (Northern Serbia) loess–paleosol sequence: revised chronostratigraphy and long-term environmental trends. Quat. Sci. Rev. 30, 1142–1154.
Marković, S.B., Hambach, U., Stevens, T., Jovanović, M., O'Hara-Dhand, K., Basarin, B., Lu, H., Smalley, I., Buggle, B., Zech, M., Svirčev, Z., Sümegi, P., Milojković, N., Zöller, L., 2012. Loess in the Vojvodina region (Northern Serbia): an essential link between European and Asian Pleistocene environments. Netherlands J. Geosci. 91 (1–2), 173–188.
Miko, S., Halamić, J., Peh, Z., Galović, L., 2001. Geochemical baseline mapping of soils developed on Diverse Bedrock from two regions in Croatia. Geol. Croat. 54 (1), 53–118.

Mikulčić Pavlaković, S., Crnjaković, M., Tibljaš, D., Šoufek, M., Wacha, L., Frechen, M., Lacković, D., 2011. Mineralogical and geochemical characteristics of quaternary sediments from the Island of Susak (Northern Adriatic, Croatia). Quat. Int. 234, 32–49.

Molnár, D., Hupuczi, J., Galović, L., Sümegi, P., 2010. Preliminary malacological investigation on the loess profile at Zmajevac, Croatia. Central Eur. J. Geosci. 2 (1), 52–56.

Muhs, D.R., Budahn, J.R., 2006. Geochemical evidence for the origin of late Quaternary loess in central Alaska. Can. J. Earth Sci. 43, 323–337.

Muhs, D.R., Budahn, J., Prospero, J.M., Carey, S.N., 2007. Geochemical evidence for African dust inputs to soils of western Atlantic islands: Barbados, the Bahamas and Florida. J. Geophys. Res. 112, F02009.

Muhs, D.R., Budahn, J.R., 2009. Geochemical evidence for African dust and volcanic ash inputs to terra rossa soils on carbonate reef terraces, northern Jamaica, West Indies. Quat. Int. 196, 13–35.

Muhs, D.R., Budahn, J., Avila, A., Skipp, G., Freeman, J., Patterson, D.A., 2010. The role of African dust in the formation of Quaternary soils on Mallorca, Spain and implications for the genesis of Red Mediterranean soils. Quat. Sci. Rev. 29, 2518–2543.

Munroe, J.S., Farrugia, G., Ryan, P.C., 2007. Parent material and chemical weathering in alpine soils on Mt. Mansfield, Vermont, USA. Catena 70, 39–48.

Munsell Soil Color Charts, 2000. Munsell Soil Color Charts. Macbeth Division of Kollmorgem Instruments Corporation, New Windsor.

Mutić, R., 1990. Korelacija kvartara istočne Slavonije na osnovi podataka mineraloško-petrografskih analiza (Istočna Hrvatska, Jugoslavija) – Dio II: Lesni ravnjak. Acta Geol. 20 (2), 29–80, Zagreb, (in Croatian).

Oreščanin, V., Lulić, S., Medunić, G., Mikelić, L., 2005. Granulometric and chemical composition of the Danube River sediments, Batina Village, Croatia. Geol. Croat. 58 (2), 185–194.

Pamić, J., Pikija, M., 1987. Badenian andesites and pyroclastics from Baranja in northern Croatia (Yugoslavia). Acta Geol. Hung. 30 (1–2), 111–132.

Pavelić, D., Kovačić, M., Vlahović, I., Wacha, L., 2011. Pleistocene calcareous aeolian–alluvial deposition in a steep relief karstic coastal belt (island of Hvar, eastern Adriatic, Croatia). Sediment. Geol. 239 (1–2), 64–79.

Peh, Z., Šajn, R., Halamić, J., Galović, L., 2008. Multiple discriminant analysis of the Drava River alluvial plain sediments. Environ. Geol. 55 (7), 1519–1535.

Poje, M., 1985. Praporne naslage "vukovarskog profila" i njihova stratigrafska pripadnost. Geol. vjesnik 38, 45–66 (in Croatian).

Poje, M., 1986. Ekološke promjene na vukovarskom prapornom ravnjaku proteklih cca 500.000 godina. Geol. vjesnik 39, 19–42 (in Croatian).

Retallack, G.J., 2001. Soils of the Past. An Introduction to Paleopedology. Blackwell Science Ltd., Oxford.

Romić, M., Bragato, G., Zovko, M., Romić, D., Mosetti, D., Galović, L., Bakić, H., 2014. The characteristics of soils developed from coastal paleosand (Korčula Island, Croatia). Catena 113, 281–291.

Rubinić, V., Durn, G., Husnjak, S., Tadej, N., 2014. Composition, properties and formation of Pseudogley on loess along a precipitation gradient in the Pannonian region of Croatia. Catena 113, 138–149.

Rubinić, V., Galović, L., Husnjak, S., Durn, G., XXXX. Climate vs. parent material – which is the key of Pseudogley diversity in Croatia? Geoderma (submitted).

Rukavina, D., 1983. O stratigrafiji gornjeg pleistocena s osvrtom na topla razdoblja i njihov odraz u naslagama na području Jugoslavije. Rad JAZU 19, 199–221, Zagreb, (in Croatian).

Smalley, I., Marković, S., Svirčev, Z., 2011. Loess is [almost totally formed by] the accumulation of dust. Quat. Int. 240, 4–11.

Smalley, I., O'Hara-Dhand, K., Kwong, J., 2014. China: materials for a loess landscape. Catena 117, 100–107.

Šajn, R., Halamić, J., Peh, Z., Galović, L., Šorša, A., 2008. Experimental geochemical map of Croatia and Slovenia. In: Schedl, A. (Ed.), 30 Jahre angewandte Geochemie in Oesterreich. Geologische Bundesanstalt 16.

Šajn, R., Halamić, J., Peh, Z., Galović, L., Alijagić, J., 2011. Assessment of the natural and anthropogenic sources of chemical elements in alluvial soils from the Drava River using multivariate statistical methods. J. Geochem. Explor. 110 (3), 278–289.

Salminen, R., Tarvainen, T., Demetriades, A., Duris, M., Fordyce, F.M., Gregorauskiene, V., Kahelin, H., Kivisilla, J., Klaver, G., Klin, H., Larson, J.O., Lis, J., Locutura, J., Marsina, K., Mjartanova, H., Mouvet, C., O'Connor, P., Ódor, L., Ottonello, G., Paukola, T., Plant, J.A., Reimann, C., Schermann, O., Siewers, U., Steenfelt, A., van der Sluys, J., de Vivo, B., Wiliams, L., 1998. FOREGS Geochemical Mapping – Field Manual Guide 47. Geological Survey of Finland, Espoo.

Salminen, R., Batista, M.J., Bidovec, M., Demetriades, A., De Vivo, B., De Vos, W., Duris, M., Gilucis, A., Gregorauskiene, V., Halamić, Josip., Heitzmann, P., Lima, A., Jordan, G., Klaver, G., Klein, P., Lis, J., Locutura, J., Marsina, K., Mazreku, A., O'Connor, P.J., Olsson, S.A., Ottesen, R.-T., Petersell, V., Plant, J.A., Reeder, S., Salpeteur, I., Sandstrom, H., Siewers, U., Steenfelt, A., Tarvainen, T., 2005. Geochemical Atlas of Europe, Part 1, Background Information, Methodology and Maps Espoo. Geological Survey of Finland.

Singhvi, A.K., Bronger, A., Sauer, W., Pant, R.K., 1989. Thermoluminescence dating of loess–paleosol sequences in the Carpathian basin (East-Central Europe): a suggestion for a revised chronology. Chem. Geol. (Isotope Science Section) 73, 307–317.

Song, Y., Chen, X., Qian, L., Li, C., Li, Y., Li, X., Chang, H., An, Z., 2014. Distribution and composition of loess sediments in the Ili Basin, Central Asia . Quat. Int. 334, 61–73.

Sun, J., Li, S.-H., Muhs, D.R., Li, B., 2007. Loess sedimentation in Tibet: provenance, processes, and link with Quaternary glaciations. Quat. Sci. Rev. 26, 2265–2280.

Taylor, S.R., Mclennan, S.M., 1995. The geochemical evolution of the continental crust. Rev. Geophys. 33 (2), 241–265.

Újvári, G., Varga, A., Balogh-Brunstad, Z., 2008. Origin, weathering, and geochemical composition of loess in southwestern Hungary. Quat. Res. 69 (3), 421–437.

Újvári, G., Varga, A., Raucsik, B., Kovács, J., 2014. The Paks loess–paleosol sequence: a record of chemical weathering and provenance for the last 800 ka in the mid-Carpathian Basin. Quat. Int. 319, 22–37.

Van Lagen, B., 1993. Manual for Chemical Soil Analyses. Department of Soil Science and Geology, Agricultural University Wageningen.

Wacha, L., Frechen, M., 2011. The chronology of the "Gorjanović loess section" in Vukovar, Croatia. Quat. Int. 240, 87–99.

Wacha, L., Mikulčić Pavlaković, S., Frechen, M., Crnjaković, M., 2011. The loess chronology of the Island of Susak, Croatia. Quat. Sci. J. (E&G) 60 (1), 153–169.

Wacha, L., Galović, L., Koloszár, L., Magyari, Á., Chikán, G., Marsi, I., 2013. The chronology of the Šarengrad II loess–paleosol section (Eastern Croatia). Geol. Croat. 66 (3), 191–203.

Yang, X.P., Zhu, B.Q., White, P.D., 2007. Provenance of aeolian sediment in the Taklamakan desert of western China, inferred from REE and major-elemental data. Quat. Int. 175, 71–85.

Yingjun, M., Congqiang, L., 1999. Trace element geochemistry during chemical weathering as exemplified by the weathered crust of granite, Longnan. Jiangxi Chin. Sci. Bull. 44 (24), 1999.

Zech, M., Marković, S., Hambach, U., Huang, Y., 2013. Humid glacials, arid interglacials? Critical thoughts on pedogenesis and paleoclimate based on multi-proxy analyses of the loess–paleosol sequence Crvenka, Northern Serbia. Palaeogeogr. Palaeoclimatol. Palaeoecol. 387, 165–175.